

# Exploring Higgs boson Yukawa interactions with a scalar singlet using Dyson-Schwinger equations

Tajdar Mufti \*

Lahore University of Management Sciences  
Sector U, D.H.A, Lahore Cantt, 54792, Pakistan

## Abstract

Higgs, being the first discovery of a fundamental scalar field in the standard model (SM), opens the possibility of existence of other scalar or pseudo scalar particles in nature. Though it does not conclusively fulfill the role of inflaton, it does provide motivation for experimental searches involving interactions of scalar (or pseudo scalar) particles as well as implications of such particles' existence from the perspective of theoretical understanding. Yukawa interactions are among the possible interactions. The considered model addresses Yukawa interaction, with various cutoff values, among the Higgs (and Higgs bar) <sup>1</sup> and a real singlet scalar field using Dyson Schwinger equations (DSEs) over a range of bare coupling values relevant to inflation-related physics for several scalar bare masses, while keeping the Higgs' mass fixed at two values for two different scenarios, without involving any DSEs but those for the field propagators. It is found that Higgs propagators are tree level dominated while scalar propagators, despite their dependence on parameter region, do not degenerate over the whole parameter space. The interaction vertices show significant deviations from tree level expression for a number of parameters and exhibit two distinct behaviors. Furthermore, the theory does not show any conclusive sign of triviality over the explored parameter space, despite suppressed vertices for some parameters, particularly for small coupling value in a certain region of parameter space.

## 1 Introduction

Higgs [1–3] sector has taken the status of a cornerstone in the standard model [4–6] after Higgs' experimental finding [7, 8]. Its very existence was indeed expected since it renders several particles in the SM, electroweak interaction bosons in particular, massive in a renormalizable manner [4, 5].

---

\*tajdar.mufti@gmail.com, tajdar.mufti@lums.edu.pk

<sup>1</sup>Higgs bar is referred to  $h^\dagger$ , with  $h$  being the Higgs field, throughout this paper.

However, implications of its existence may very well reach far beyond low energy phenomenology of the standard model [5], supersymmetry [9] and cosmology [10, 11] being two of these examples. It also opens a possibility of existence of a whole scalar sector to be experimentally discovered and studied from the perspectives of both theory and phenomenology.

In supersymmetry [9], implications of scalar fields as fundamental degrees of freedom are beyond a mass generating mechanism which was indeed one of the reasons for frantic SM Higgs-related searches over past few decades. There can be found a plethora of reports, for instance [12], suggesting a number of scalars providing various extensions to the already known SM [13], and even to cosmological scenarios [14]. In particular, in minimal supersymmetric models Higgs boson is expected to be smaller than 135 GeV [3, 15–18] which turns out to be the correct prediction [7, 8]. However, as experimental searches [19, 20] are yet to confirm their existence in nature, the status of supersymmetry remains inconclusive to this day.

In cosmology, Higgs was suspected to cause inflation [11, 21, 22], which in recent years revived interest in Higgs related cosmology [23, 24]. However, as the quartic self coupling of Higgs is found to be around 0.6 [25], which is significantly different than what was expected to produce slow rolling during cosmic inflation [10, 25, 26], it is reasonable to expect at least one more scalar field required by current understanding of inflation [27]. As the experimental discovery [7, 8] places Higgs as the only fundamental scalar field in the standard model, it presents an opportunity to explore interactions among scalar (or pseudo scalar) fields using experimentally known results from Higgs searches.

Furthermore, relevance of Higgs physics in areas beyond cosmic inflation and supersymmetry has also been studied as the involving interactions are important from several aspects including possible extension of the SM, see for example [28–30].

As for the case of Higgs, interactions of a scalar singlet field have also been studied at length from various perspectives, a similar theory studied being [31], particularly dark matter physics [32–37]. Though, the  $\phi^4$  theory is found to be a trivial theory [38–45], it has not been yet established if its interactions with other fields also render the theories trivial. For the case of Higgs, which is also a (complex doublet) scalar field, its interactions with gauge fields [46], have not shown any conclusive sign of triviality, which supports assuming scalar interactions non-trivial unless proven otherwise for a model.

In this paper Yukawa interaction between Higgs and a real scalar singlet is studied using Dyson Schwinger equations <sup>2</sup> [47–51]. The studies is conducted under the paradigm of quantum field theory with flat background

---

<sup>2</sup>Throughout this paper, Higgs is referred to the doublet complex scalar field, and scalar field is reserved for scalar singlet field.

and coupling values of the order relevant to physics related to inflation [25]. The theory is explored in terms of propagators, vertices, and cutoff effects. Higgs masses are set at 125.09 GeV [7, 8, 52, 53], and 160 GeV [54]. The theory is studied with different scalar (bare) masses from electroweak to TeV regime <sup>3</sup>. There is a companion paper which takes into account other renormalizable interaction vertices [55] covering a larger parameter space <sup>4</sup>, though using a different numerical approach [56], and a paper which addresses phenomenology and further generalized results of the same theory [57].

At this point, the theory does not contain any four point self interactions in the Lagrangian. As the Yukawa interaction term in the theory can also produce 4 point self interactions for both Higgs and scalar fields, these self interactions are not included in the Lagrangian in favor of, seemingly more fundamental, three point Yukawa interaction. Inclusion of these four point self interactions are considered somewhere else [55].

The model considered here is a variant of Wick-Cutkosky model [58] which has been studied in different contexts [59–61]. A significant part of such studies takes into account real, massive as well as massless, singlet scalar self interacting fields via a three point interaction vertex [31]. Two scalar fields under the same model have also been studied under the same model [62]. However, most of these studies have various kinds of assumptions used to either study different aspects or applications of the model or solve the theory exactly. In this paper no additional assumptions have been used in numerically extracting the correlation functions which are to be used to calculate further quantities related to Higgs phenomenology [57]. The only prominent constraints are renormalization conditions on the two and three correlation functions, which are among the typical features of, particularly phenomenology related, quantum field theories, and a condition to suppress local numerical fluctuations as mentioned below. In addition, fixing of a parameter during renormalization is implemented, as mentioned below, which is not strictly a constraint as it can be allowed in a QFT.

## 2 Technical Details

The theory is explored using approach of Dyson Schwinger equations [50, 63] in Euclidean space. The (bare form of) Lagrangian is given by

$$L = \delta^{\mu\nu} \partial_\mu h^\dagger \partial_\nu h + m_h^2 h^\dagger h + \frac{1}{2} \delta^{\mu\nu} \partial_\mu \phi \partial_\nu \phi + \frac{1}{2} m_s^2 \phi^2 + \lambda \Pi \phi h^\dagger h \quad (1)$$

---

<sup>3</sup>Throughout the paper, electroweak regime is taken as  $m_s$  from 1 GeV to 600 GeV, while TeV regime refers to above 600 GeV values.

<sup>4</sup>This study is being conducted in the presence of four point interactions, hence containing the current parameter space as a sub space.

with Higgs fields (h) with SU(2) symmetry and  $\phi$  a real singlet scalar field.  $\Pi$  is a dimensionful parameter used to render  $\lambda$  dimensionless. For the current investigation  $\Pi$  is set to 1 GeV. Since  $\Pi$  here is a non-dynamic parameter,  $\lambda$  is used throughout this paper instead of the coupling  $\lambda_e = \lambda\Pi$ <sup>5</sup>. As mentioned above, and to discern implications of Yukawa coupling in the theory with the numerical set up of computations presented below, all interactions higher than 3 field interaction have been kept from the Lagrangian.

Dyson Schwinger equations (in unrenormalized form) for propagators,  $H^{ij}(p)$  for Higgs and  $S(p)$  for scalar singlet fields, respectively, in momentum space are given by

$$H^{ij}(p)^{-1} = \delta^{ij}(p^2 + m_h^2) + 2\lambda_e \int \frac{d^4q}{(2\pi)^4} S(q) \Gamma^{ik}(-p, p-q, q) H^{kj}(q-p) \quad (2)$$

$$S(p)^{-1} = p^2 + m_s^2 + \lambda_e \int \frac{d^4q}{(2\pi)^4} H^{ik}(q) \Gamma^{kl}(q, p-q, -p) H^{li}(q-p) \quad (3)$$

with  $\Gamma^{kl}(u, v, w)$  being the three point Yukawa interaction vertex of Higgs, Higgs bar, and scalar fields with momentum u, v, and w, respectively. Higgs and Higgs bar fields have indices k and l, respectively. The renormalization conditions for the propagators [63] are

$$H^{ij}(p)|_{p^2=m_h^2} = \frac{\delta^{ij}}{p^2 + m_h^2}|_{p^2=m_h^2} \quad (4)$$

$$S(p)|_{p^2=m_s^2} = \frac{1}{p^2 + m_s^2}|_{p^2=m_s^2} \quad (5)$$

Details of renormalization procedure is given later in the subsection. The starting expressions of correlation functions for numerical computations are set to their tree level expressions. For every update of vertex and propagators, Newton Raphson's method is implemented locally. Higgs propagators are also updated using the same method while scalar propagators are calculated directly from the respective DSE with renormalization procedure implemented. Hence, under the boundary conditions the propagators are updated or calculated from the respective DSE, and the vertex is updated to numerically evolve towards a solution such that both equations are satisfied within the preselected size of local error. Uniqueness of solutions is implicitly assumed.

As there are three unknown correlation functions, a commonly used approach is to use a third DSE for the interaction vertex. However, it introduces (most likely) unknown, further higher correlation function(s) depending upon the theory. This never ending sequence is coped with truncations and assumptions [50, 63]. Several approaches (such as ladder approximation)

---

<sup>5</sup>From this point, the word *coupling* is reserved for  $\lambda$  throughout the current report.

are commonly used for studies involving DSEs. Some of these approaches may still be numerically suitable and economical, as the unknown higher correlation functions are replaced by suitable assumptions, such as modeling them in terms of other lower correlation functions. However, the resulting correlation functions may be effected by such truncations and modeling. On the contrary, during the current investigation only the renormalization conditions for propagators and the vertex (and fixing of a parameter) are used which, along with their symmetry properties imposed by the physics and the integral equations, act as constraints on the vertex. Hence, two non-linear coupled integral equations make it possible to extract three unknown correlation functions without resorting to conventionally employed means stated above, and only the interplay of the quantities within the theory is made the most of.

The computations are performed to achieve correlation functions with less than  $10^{-20}$  local uncertainties in results <sup>6</sup>. All results are for the vertices formed by Higgs and scalar fields with momentum perpendicular to each other, while the other Higgs (bar) field carries the momentum obeying standard conservation principles.

Suppression of local fluctuations in vertex is numerically implemented by requiring that local fluctuations never exceed by an order of magnitude in (Euclidean) space-time. In addition, there are two measures taken in algorithms to stabilize the correlation functions, particularly the vertex as there is no separate DSE for the vertex. First, updates of correlation functions is based on sum of the squared errors in the DSE of Higgs propagator, instead of local error [50]. It slows the computation but contributes in extracting a numerically stable vertex. Secondly, for the Higgs propagators the following polynomial representation is introduced.

$$H^{ij}(p) = \delta^{ij} \frac{\sum_{i=0}^N a_i p^{2i}}{p^2 + m^2 + \sum_{l=0}^N b_l p^{2l}} \quad (6)$$

The parameters  $a_i$  and  $b_l$  are updated numerically during computations. The advantage is that, while allowing freedom to Higgs propagators within the renormalization scheme and symmetries of the two DSEs, it further contributes in restraining the self energy terms and, hence, stabilizing the vertex. Another advantage of such an implementation is time efficiency in comparison to implementing other numerical approaches, such as interpolation. However, no representation is used for either scalar propagator or the vertex as it was found to severely effect the numerical precision and

---

<sup>6</sup>As uncertainties are lower than the mentioned magnitude, the error bars in the diagrams included in the paper are not visible.

time efficiency. Thus, starting with the tree level structures, above mentioned measures immensely facilitate during computation of the correlation functions in the theory.

The parameters for computations have been chosen to either explore the dynamics in the theory in both perturbative and non-perturbative regimes in the context of studies of richer theories [55, 64], or their relevance to phenomenology. Higgs masses have been chosen with inspiration from the discovery of Higgs [7, 8] as well as studies of heavy Higgs scenarios [46, 65]. In total, 144 sets of parameters are studied with  $10^{-3} \leq \lambda \leq 2.0$  and  $1.0 \text{ GeV} \leq m_s \leq 2.5 \text{ TeV}$ , for  $m_h = 125.09 \text{ GeV}$  and  $m_h = 160 \text{ GeV}$ .

The order of coupling values have been chosen regarding the quartic coupling value for inflationary scenarios involving Higgs [25]. As Feynman's box diagrams containing only three point Yukawa interaction can also represent four point self interactions for both Higgs and scalar fields, it is assumed that fourth power of Yukawa bare coupling can naively represent a bare 4 point self interaction coupling, and the above mentioned range of bare coupling values becomes natural choice for such explorations.

The theory was investigated with 5 TeV, 20 TeV, 40 TeV, and 60 TeV as cutoff values in order to explore cutoff effects.

Gaussian quadrature algorithm is used for numerical integration.

## 2.1 Renormalization Procedure

The renormalization procedure implemented in the equation of scalar propagator is as follows: Adding the counter terms in the Lagrangian in equation 1, equation 3 becomes

$$S_r(p)^{-1} = (1 + A)p^2 + m_s^2 + B + \lambda \int \frac{d^4 q}{(2\pi)^4} H_r^{ik}(q) \Gamma_r^{kl}(q, p - q, -p) H_r^{li}(q - p) \quad (7)$$

where A, and B are real constants, r is the subscript for renormalized terms, and

$$\Gamma_r^{kl}(q, p - q, -p) = (1 + \frac{C}{\lambda}) \Gamma^{kl}(q, p - q, -p) \quad (8)$$

with C also a real constant <sup>7</sup>. Similarly, for the case of the Higgs propagator, equation 2 takes the form

$$H^{ij}(p)^{-1} = \delta^{ij}((1 + \alpha)p^2 + m_h^2 + \beta) + 2\lambda \int \frac{d^4 q}{(2\pi)^4} S(q) \Gamma_r^{ik}(-p, p - q, q) H^{kj}(q - p) \quad (9)$$

---

<sup>7</sup>There is no *running* coupling in this case because the contributions in coupling beyond the bare value are absorbed in the definition of the vertex.

with  $\alpha$  and  $\beta$  as the constants due to the counter terms. Without imposing any strong constraints, parameters  $B$  and  $\beta$  are defined as,

$$\begin{aligned} B &= Am_s^2 + 2\lambda(1+A)(1+\alpha)\sigma_s \\ \beta &= \alpha m_h^2 + 2\lambda(1+A)(1+\alpha)\sigma_h \end{aligned} \quad (10)$$

with  $\sigma_s$  and  $\sigma_h$  as the parameters to be determined during computations.  $\Gamma_r^{ab}(p, -p-q, q)$  are also defined as

$$\Gamma_r^{ab}(p, -p-q, q) = (1+A)(1+\alpha)\tilde{\Gamma}_r^{ab}(p, -p-q, q) \quad (11)$$

As counter terms are introduced for every term in the Lagrangian, it introduces one unknown parameter for each term [66]. Thus, it is assumed that rescaling the Lagrangian (with counter terms) does not change the physics because the action of the theory becomes invariant upon an appropriate rescaling of (the differentials of) spacetime. It naturally, gives freedom to set one of the unknown parameters introduced upon inserting the counter terms in the theory. Hence,  $\alpha$  is set to 0.

In addition, as mass of the Higgs boson is already known, the renormalized (squared) mass of the Higgs boson ( $m_{h,r}^2$ ) is fixed at 125.09 GeV, and 160.0 GeV as a test case of heavy Higgs <sup>8</sup>. Hence, the DSEs (with  $\alpha = 0$ ) to be used for computations are

$$S_r(p)^{-1} = (1+A)(p^2 + m_s^2 + 2\lambda\sigma_s + I_s(p)) \quad (12)$$

and

$$H_r^{ij}(p)^{-1} = \delta^{ij}(p^2 + m_{h,r}^2) + I_h^{ij}(p) \quad (13)$$

where

$$I_s(p) = \lambda \int \frac{d^4q}{(2\pi)^4} H_r^{ik}(q) \tilde{\Gamma}_r^{kl}(q, p-q, -p) H_r^{li}(q-p) \quad (14)$$

$$I_h^{ij}(p) = 2\lambda(1+A) \int \frac{d^4q}{(2\pi)^4} S(q) \tilde{\Gamma}_r^{ik}(-p, p-q, q) H_r^{kj}(q-p) \quad (15)$$

Only the flavor diagonal Higgs propagators are assumed to be non-zero, as is the case for the tree level Higgs propagators. In order to suppress ambiguities between  $\sigma_s$  and the vertex during numerical convergence,  $\tilde{\Gamma}_r^{ab}(p, -p-q, q)$  is fixed to coupling constant at the highest momentum value.

## 3 Propagators

### 3.1 Scalar Propagators

Scalar propagator is, despite that they are calculated using Higgs propagators and interaction vertex, found to be a highly informative quantity in the

---

<sup>8</sup>Since Higgs mass is kept fixed at its renormalized value, notations  $m_h$  and  $m_{h,r}$  are used interchangeably as they do not cause any confusion.

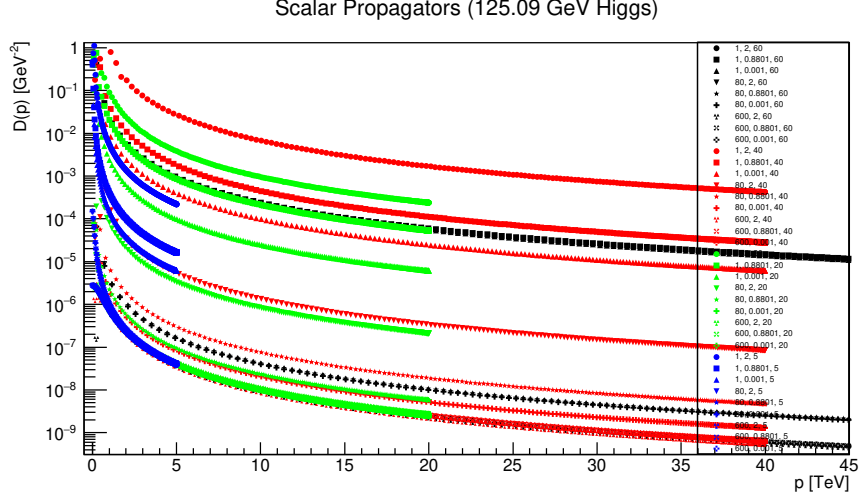


Figure 1: Scalar propagators (on logarithmic scale) for  $m_h = 125.09$  GeV are plotted (in electroweak regime) with  $1 \text{ GeV} \leq m_s \leq 600 \text{ GeV}$ ,  $0.001 \leq \lambda \leq 2.0$ , and  $5 \text{ TeV} \leq \Lambda \leq 60 \text{ TeV}$ , shown as  $(m_s, \lambda, \Lambda)$  on the figure.

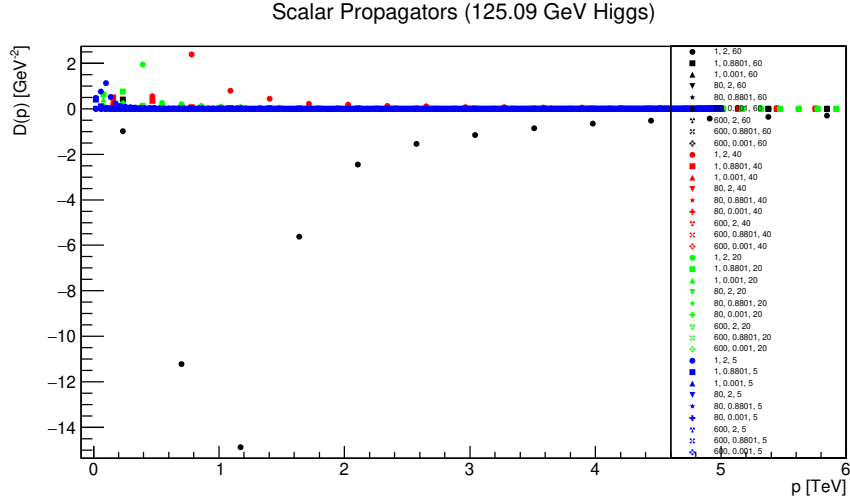


Figure 2: Scalar propagators for  $m_h = 125.09$  GeV are plotted (in electroweak regime) with  $1 \text{ GeV} \leq m_s \leq 600 \text{ GeV}$ ,  $0.001 \leq \lambda \leq 2.0$ , and  $5 \text{ TeV} \leq \Lambda \leq 60 \text{ TeV}$ , shown as  $(m_s, \lambda, \Lambda)$  on the figure. Low magnitudes of propagators are highlighted.

model. Its DSE involves the constants to be known while implementing the renormalization procedure during numerical computations. The propagators are shown in figures 1, 2, 3, 6, 7, and 8.

An immediate observation is that at the ultraviolet end scalar propagators have the same qualitative behavior for both of the physical masses of



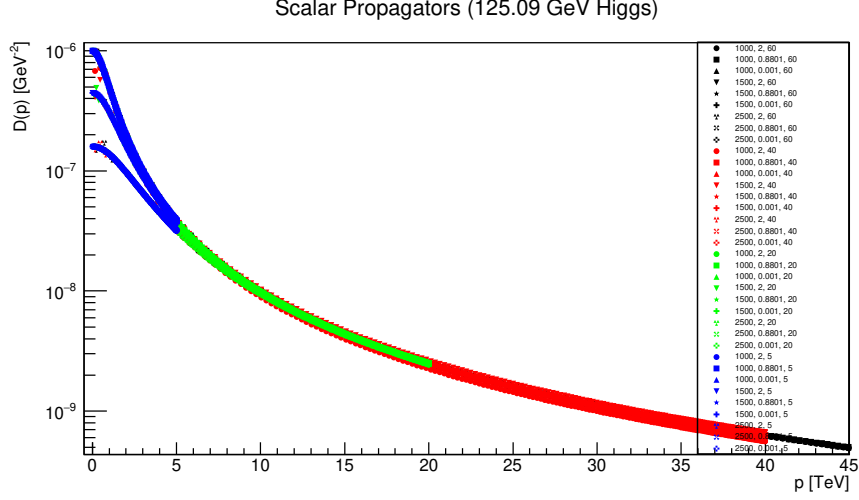


Figure 3: Scalar propagators (on logarithmic scale) for  $m_h = 125.09$  GeV are plotted (in TeV regime) with  $1000 \text{ GeV} \leq m_s \leq 2500 \text{ GeV}$ ,  $0.001 \leq \lambda \leq 2.0$ , and  $5 \text{ TeV} \leq \Lambda \leq 60 \text{ TeV}$ , shown as  $(m_s, \lambda, \Lambda)$  on the figure.

Higgs<sup>9</sup>. It becomes clear that at this end scalar self energies, defined by equation 14 should have lost any significant dependence for higher momentum while the quantitative differences appear due to the renormalization parameter  $A$  in equation 7 which is corroborated by the self energies plotted in figures 4 and 5 for  $m_h = 125.09$  GeV, and 9 and 10 for  $m_h = 160.0$  GeV, respectively.

An important observation is that for higher coupling and the lowest scalar bare mass,  $m_s = 1 \text{ GeV}$ , the propagators exhibit a tendency of having a pole, see figures 2 and 7 in which the propagators are shown without a log scale. This peculiar behavior suggests that in the model it is possible for scalars to have a negative renormalized squared mass which, as in standard literature, is taken as a sign of symmetry breaking. For the corresponding parameters, scalar self energies also show relatively pronounced negative contributions. Several other parameters are also found to have this tendency, though it is mild and suppressed for lower cutoff values, which indicates that if such a phenomenon really exists in the model, it may take place for higher cutoff values<sup>10</sup>.

Another observation for the  $m_s$  in electroweak regime is the sensitivity on parameters and cutoff. Though, several of the scalar propagators are indeed found to have similar magnitude in the infrared region, the distinction

<sup>9</sup>Throughout the current paper, physical mass and renormalized mass are used interchangeably.

<sup>10</sup>Further higher values of cutoff were not studied as it would compromise the resolution in momentum values.

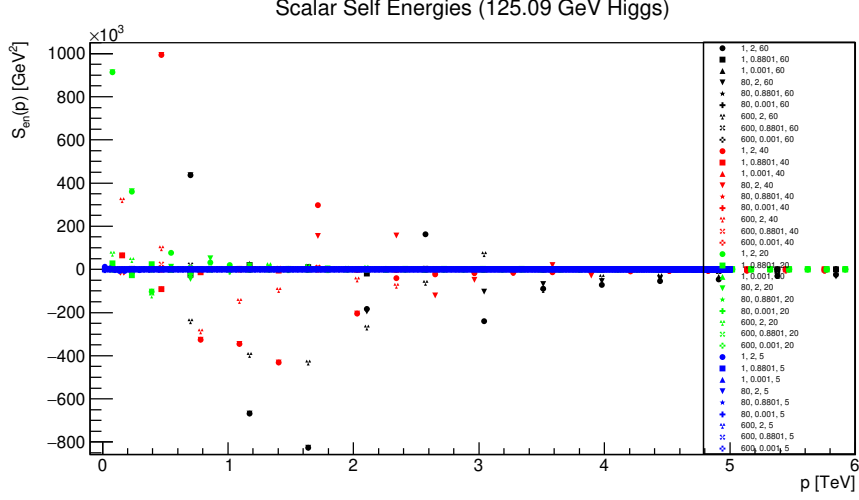


Figure 4: Scalar self energies for  $m_h = 125.09$  GeV are plotted (in electroweak regime) with  $1 \text{ GeV} \leq m_s \leq 600 \text{ GeV}$ ,  $0.001 \leq \lambda \leq 2.0$ , and  $5 \text{ TeV} \leq \Lambda \leq 60 \text{ TeV}$ , shown as  $(m_s, \lambda, \Lambda)$  on the figure.

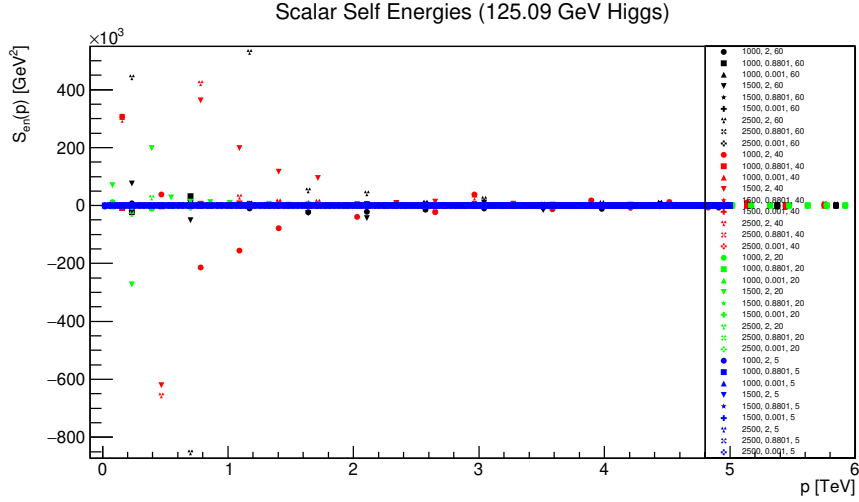


Figure 5: Scalar self energies for  $m_h = 125.09$  GeV are plotted (in TeV regime) with  $1000 \text{ GeV} \leq m_s \leq 2500 \text{ GeV}$ ,  $0.001 \leq \lambda \leq 2.0$ , and  $5 \text{ TeV} \leq \Lambda \leq 60 \text{ TeV}$ , shown as  $(m_s, \lambda, \Lambda)$  on the figure.

is evident on the figures 2 and 7, which may arise due to different values of the  $A$  parameters as mentioned above. It was also observed for a number of parameters in electroweak regime, particularly for 125.09 GeV Higgs and very low scalar bare mass, that lower the cutoff more suppressed the propagator may appear. Furthermore, in electroweak regime scalar propagators with lower cutoff are found to suffer relative suppression for a number of

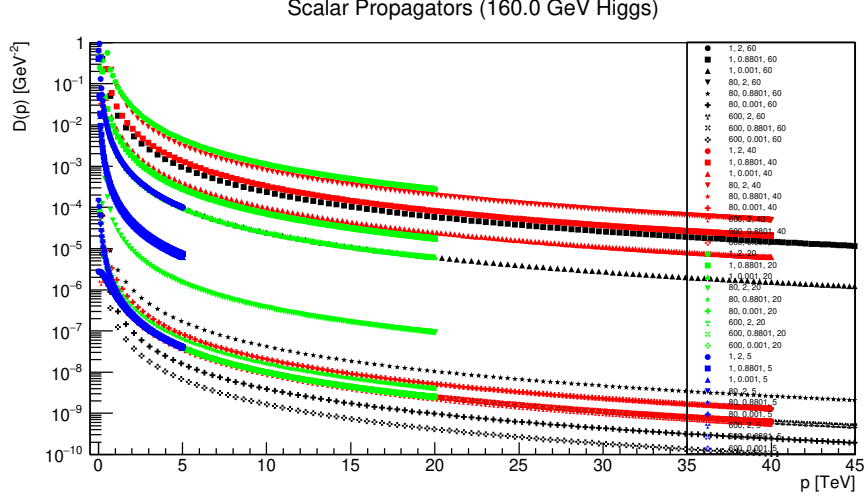


Figure 6: Scalar propagators (on logarithmic scale) for  $m_h = 160.0$  GeV are plotted (in electroweak regime) with  $1 \text{ GeV} \leq m_s \leq 600 \text{ GeV}$ ,  $0.001 \leq \lambda \leq 2.0$ , and  $5 \text{ TeV} \leq \Lambda \leq 60 \text{ TeV}$ , shown as  $(m_s, \lambda, \Lambda)$  on the figure.

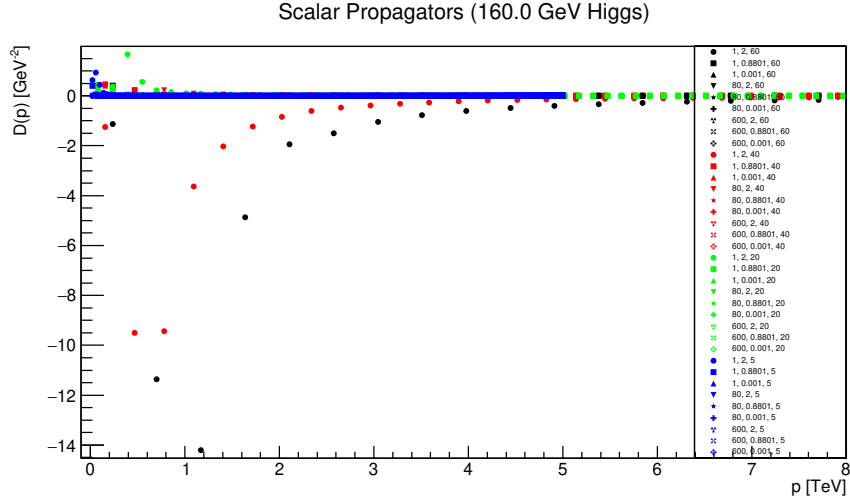


Figure 7: Scalar propagators for  $m_h = 160.0$  GeV are plotted (in electroweak regime) with  $1 \text{ GeV} \leq m_s \leq 600 \text{ GeV}$ ,  $0.001 \leq \lambda \leq 2.0$ , and  $5 \text{ TeV} \leq \Lambda \leq 60 \text{ TeV}$ , shown as  $(m_s, \lambda, \Lambda)$  on the figure. Low magnitudes of propagators are highlighted.

parameters.

For  $m_s$  in TeV regime, the propagators manifest differently than in electroweak regime. First of all, instead of having a variety of propagators they are extremely close to each other beyond (approximately) 10 TeV momentum. Hence, infrared region is more interesting than the ultraviolet region.

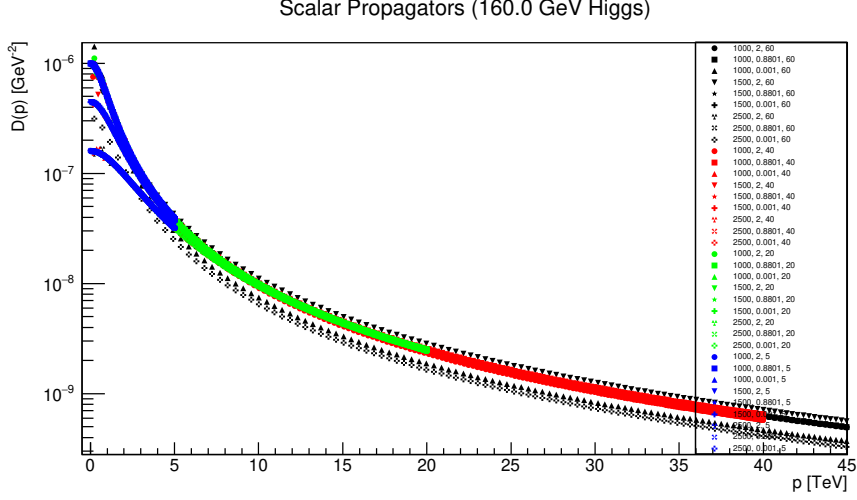


Figure 8: Scalar propagators (on logarithmic scale) for  $m_h = 160.0$  GeV are plotted (in TeV regime) with  $1000 \text{ GeV} \leq m_s \leq 2500 \text{ GeV}$ ,  $0.001 \leq \lambda \leq 2.0$ , and  $5 \text{ TeV} \leq \Lambda \leq 60 \text{ TeV}$ , shown as  $(m_s, \lambda, \Lambda)$  on the figure.

In this region, instead of a wide variety as in case of electroweak regime the propagators are found to accumulate in groups, see figure 3. For higher Higgs mass ( $m_h = 160$  GeV), scalar propagators are found to have dependence on parameter space to some extent, see figure 8, but qualitatively the propagators manifest in the similar way as for light Higgs case ( $m_h = 125.09$  GeV) due to the A parameter in the renormalized form of DSE for scalar propagator. Their qualitatively similar behavior indicates less deviations among the magnitudes of physical scalar masses in the regime because the A parameter only rescales the propagators in compliance with the renormalization condition in equation 5. A notable observation is suppression of propagators for higher masses and the highest cutoff value ( $\Lambda = 60$  TeV).

Scalar propagators for both Higgs masses are found to be qualitatively similar, though with limited dependence on parameter space as well as cutoff. In figures 11 and 12, renormalization parameter A for scalar propagator in the form of the quantity  $\tilde{A} = 1 + A$  is shown for various cutoff values and parameters of the theory. For higher values of  $m_s$ , irrespective of  $m_{h,r}$ , the parameter  $\tilde{A}$  is close to 1.0 which indicates small contribution of A parameter during renormalization. It suggests that the deviations in scalar propagators in the infrared region is mostly due to the contributions from self energies. However, for the values of  $m_s$  lower than 100 GeV, deviations from unity is relatively more prominent. It suggests emergence of a different behavior peculiar for smaller scalar bare masses in contrast to TeV regime.

Overall, beyond the infrared region where the deviations are prominent, scalar propagators are generally found to have (decreasing) monotonic be-

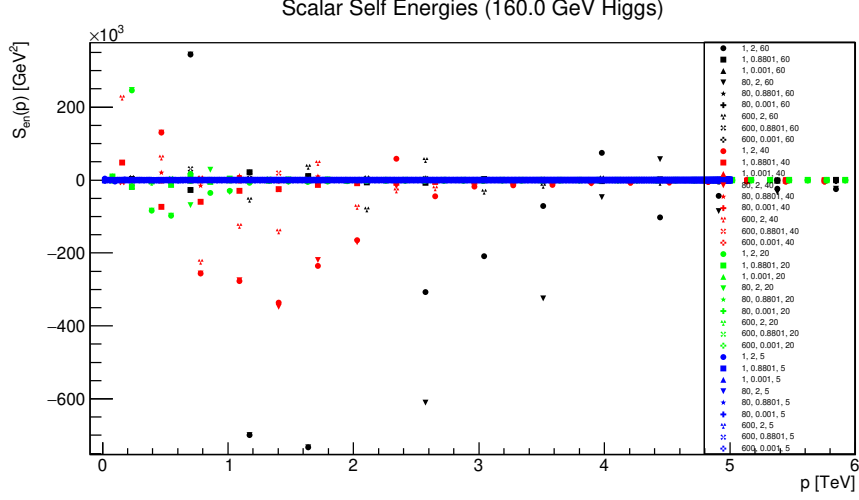


Figure 9: Scalar self energies for  $m_h = 160.0$  GeV are plotted (in electroweak regime) with  $1 \text{ GeV} \leq m_s \leq 600 \text{ GeV}$ ,  $0.001 \leq \lambda \leq 2.0$ , and  $5 \text{ TeV} \leq \Lambda \leq 60 \text{ TeV}$ , shown as  $(m_s, \lambda, \Lambda)$  on the figure.

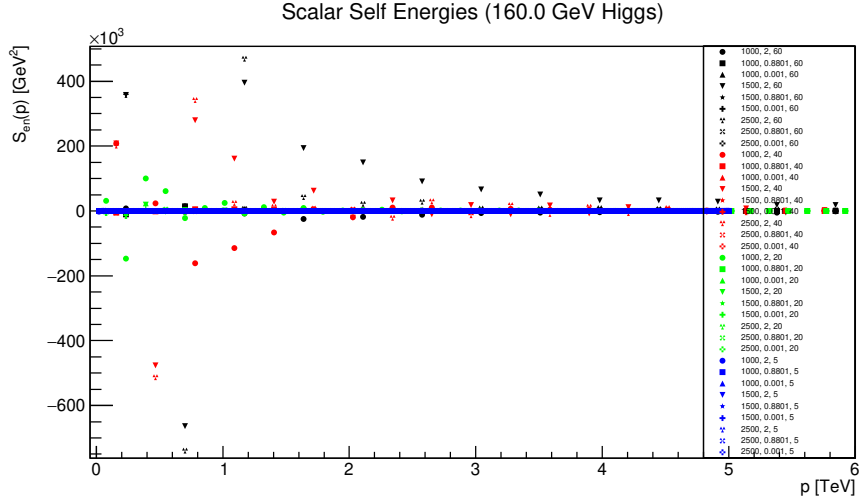


Figure 10: Scalar self energies for  $m_h = 160.0$  GeV are plotted (in TeV regime) with  $1000 \text{ GeV} \leq m_s \leq 2500 \text{ GeV}$ ,  $0.001 \leq \lambda \leq 2.0$ , and  $5 \text{ TeV} \leq \Lambda \leq 60 \text{ TeV}$ , shown as  $(m_s, \lambda, \Lambda)$  on the figure.

havior which is an indicative of a physical particle in the theory.

### 3.2 Higgs Propagators

Unlike scalar propagators, Higgs propagators are independently updated with the renormalization condition in equation 4 by updating the coefficients

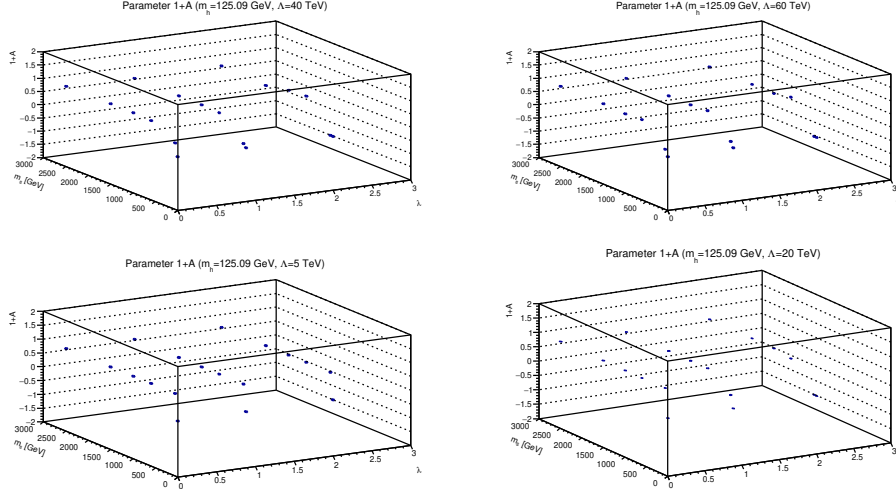


Figure 11: Renormalization quantity  $1+A$  for scalar propagator with  $m_h = 125.09$  GeV are plotted for different scalar bare masses  $m_s$  and bare couplings  $\lambda$  at different cutoff values  $\Lambda$ .

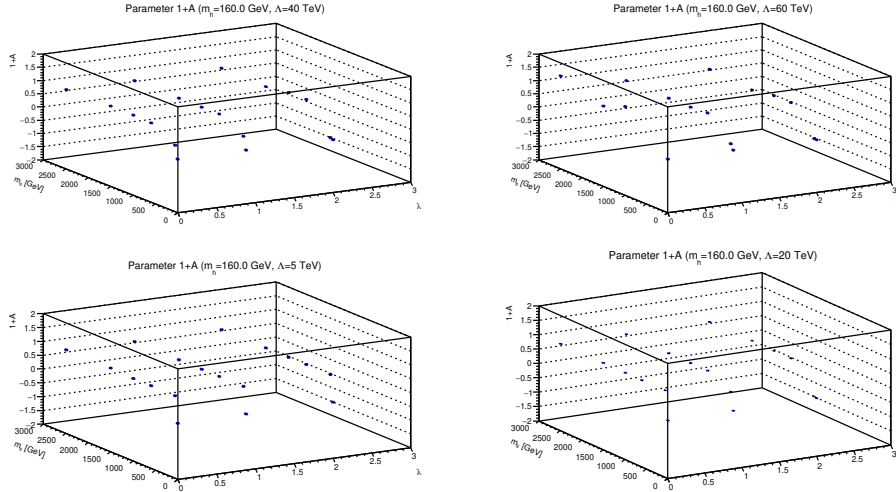


Figure 12: Renormalization quantity  $1+A$  for scalar propagator with  $m_h = 160.0$  GeV are plotted for different scalar bare masses  $m_s$  and bare couplings  $\lambda$  at different cutoff values  $\Lambda$ .

in the expansion of Higgs propagators given in equation 6. Thus, as the constant  $\alpha$  in equation 9 and the Higgs mass is kept fixed, the vertex remains the only unknown correlation beside Higgs propagators in equation 9, while the parameter  $A$  is calculated directly from the DSE of scalar propagator in equation 12.

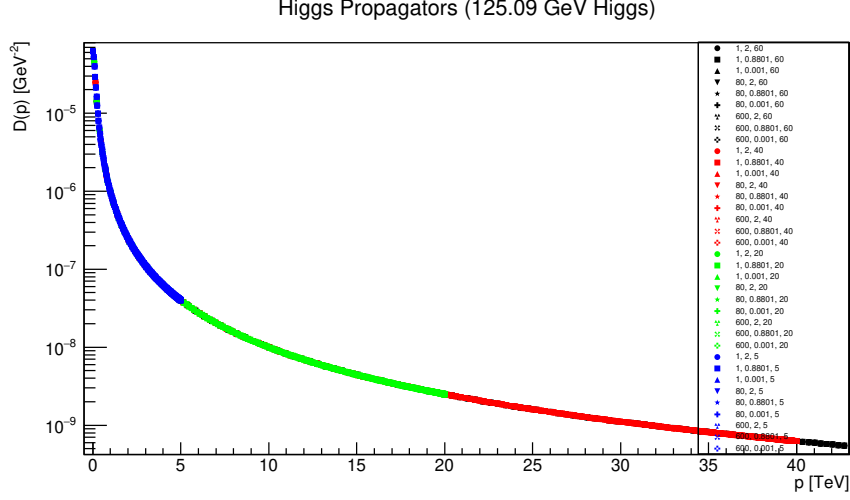


Figure 13: Higgs propagators (on logarithmic scale) for  $m_h = 125.09$  GeV are plotted (in electroweak regime) with  $1 \text{ GeV} \leq m_s \leq 600 \text{ GeV}$ ,  $0.001 \leq \lambda \leq 2.0$ , and  $5 \text{ TeV} \leq \Lambda \leq 60 \text{ TeV}$ , shown as  $(m_s, \lambda, \Lambda)$  on the figure.

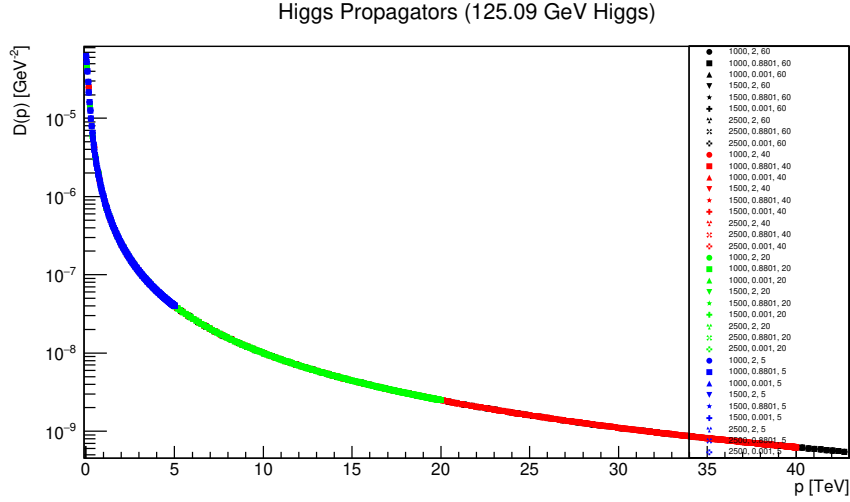


Figure 14: Higgs propagators (on logarithmic scale) for  $m_h = 160.0$  GeV are plotted (in TeV regime) with  $1000 \text{ GeV} \leq m_s \leq 2500 \text{ GeV}$ ,  $0.001 \leq \lambda \leq 2.0$ , and  $5 \text{ TeV} \leq \Lambda \leq 60 \text{ TeV}$ , shown as  $(m_s, \lambda, \Lambda)$  on the figure.

Higgs propagators for  $m_h = 125.09$  GeV are shown in figures 13 and 14 for different parameters of the theory at 4 cutoff values. An immediate observation is strong insensitivity of Higgs propagators over bare scalar masses, couplings as well as cutoff values. As the propagators manifest very close to the tree level propagators, it is a monotonically decreasing function, which indicates a physical particle. Similar situation is observed for

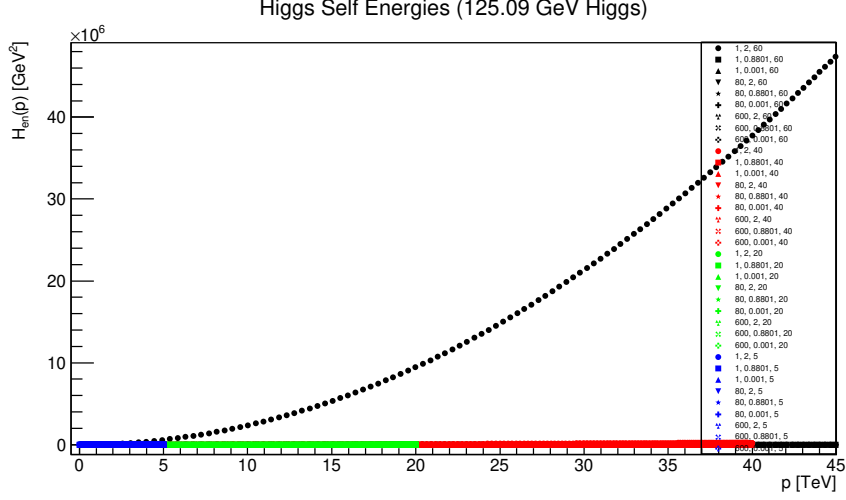


Figure 15: Higgs self energies for  $m_h = 125.09$  GeV are plotted (in electroweak regime) with  $1 \text{ GeV} \leq m_s \leq 600 \text{ GeV}$ ,  $0.001 \leq \lambda \leq 2.0$ , and  $5 \text{ TeV} \leq \Lambda \leq 60 \text{ TeV}$ , shown as  $(m_s, \lambda, \Lambda)$  on the figure.

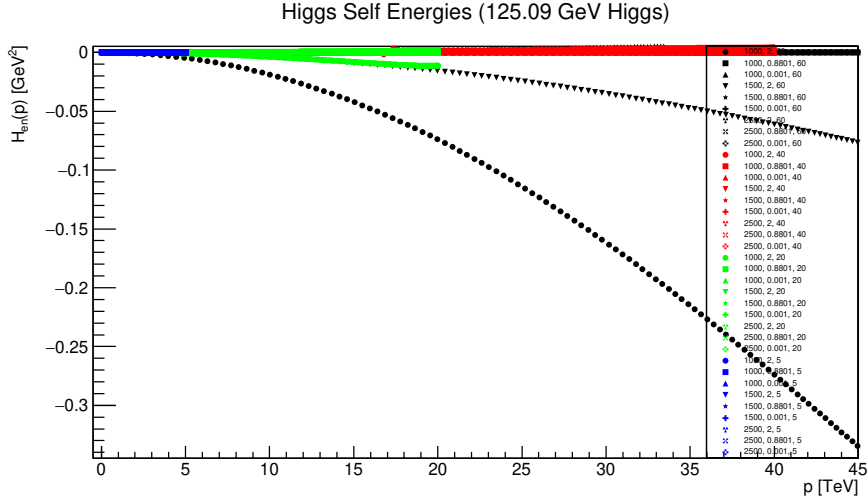


Figure 16: Higgs self energies for  $m_h = 125.09$  GeV are plotted (in TeV regime) with  $1000 \text{ GeV} \leq m_s \leq 2500 \text{ GeV}$ ,  $0.001 \leq \lambda \leq 2.0$ , and  $5 \text{ TeV} \leq \Lambda \leq 60 \text{ TeV}$ , shown as  $(m_s, \lambda, \Lambda)$  on the figure.

$m_h = 160.0$  GeV as shown in figures 17 and 18. This is also observed for the SM Higgs boson which has low contributions beyond tree level. However, what is peculiar in this model is significantly smaller, than in the SM Higgs case, contributions from self energies.

Higgs self energy terms are plotted in figures 15 and 16 for  $m_h = 125.09$  GeV, and 19 and 20 for  $m_h = 160.0$  GeV. It is observed that, though there



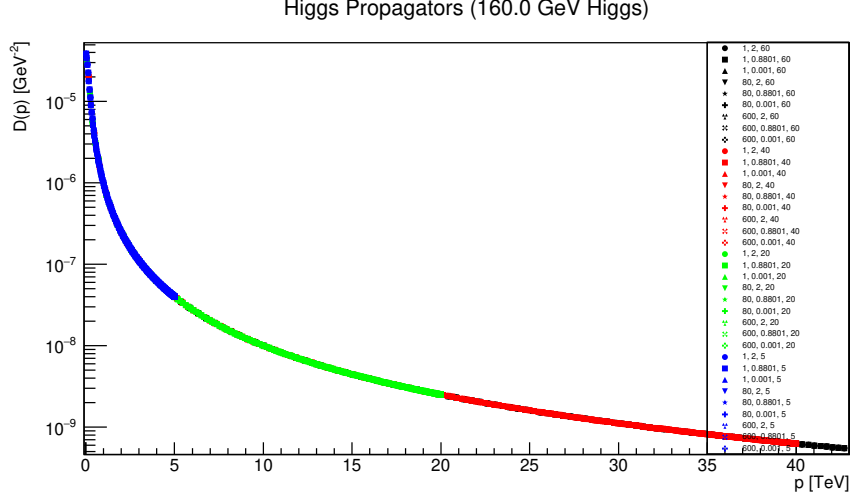


Figure 17: Higgs propagators (on logarithmic scale) for  $m_h = 160.0$  GeV are plotted (in electroweak regime) with  $1 \text{ GeV} \leq m_s \leq 600 \text{ GeV}$ ,  $0.001 \leq \lambda \leq 2.0$ , and  $5 \text{ TeV} \leq \Lambda \leq 60 \text{ TeV}$ , shown as  $(m_s, \lambda, \Lambda)$  on the figure.

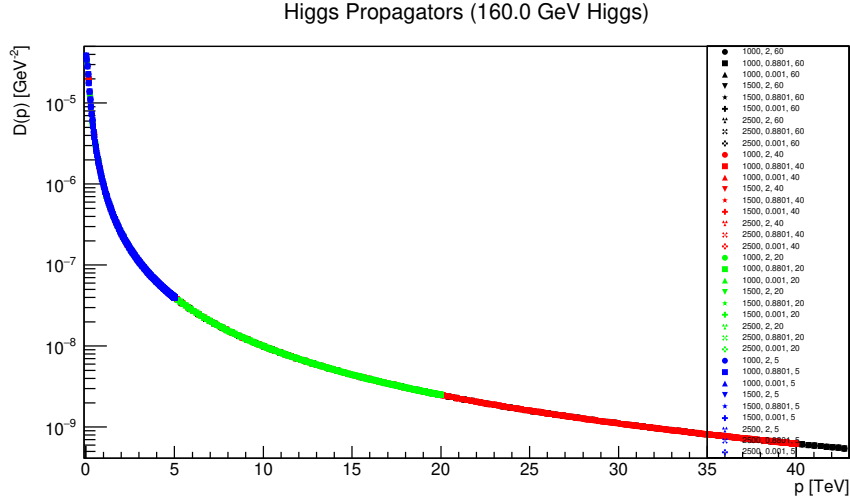


Figure 18: Higgs propagators (on logarithmic scale) for  $m_h = 160.0$  GeV are plotted (in TeV regime) with  $1000 \text{ GeV} \leq m_s \leq 2500 \text{ GeV}$ ,  $0.001 \leq \lambda \leq 2.0$ , and  $5 \text{ TeV} \leq \Lambda \leq 60 \text{ TeV}$ , shown as  $(m_s, \lambda, \Lambda)$  on the figure.

exists no competition between the contribution from self energies and the tree level structure  $(p^2 + m_h^2)$ , there is indeed a certain dependence which is relatively more distinct for higher coupling values,  $\lambda = 2.0$  is shown in the figures. A general observation is that Higgs self energies increase with momentum values if there is any dependence. However, despite that Higgs self energies can compete with (squared) Higgs mass, they are still restrained

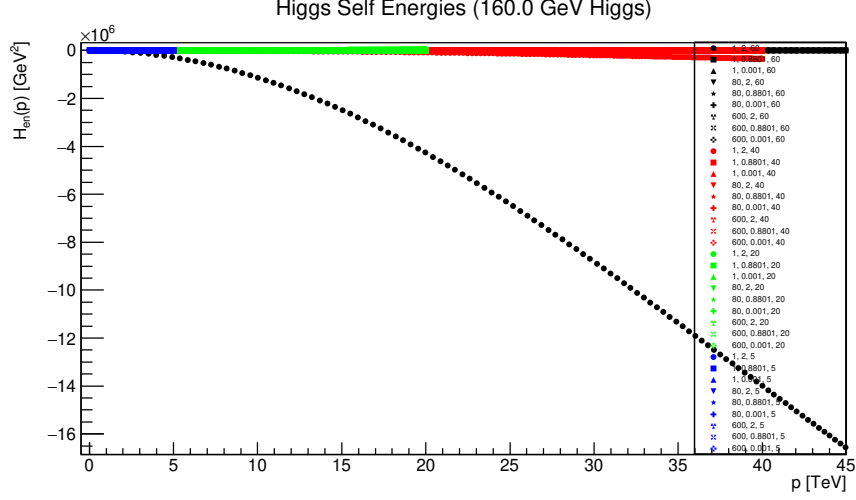


Figure 19: Higgs self energies for  $m_h = 160.0$  GeV are plotted (in electroweak regime) with  $1 \text{ GeV} \leq m_s \leq 600 \text{ GeV}$ ,  $0.001 \leq \lambda \leq 2.0$ , and  $5 \text{ TeV} \leq \Lambda \leq 60 \text{ TeV}$ , shown as  $(m_s, \lambda, \Lambda)$  on the figure.

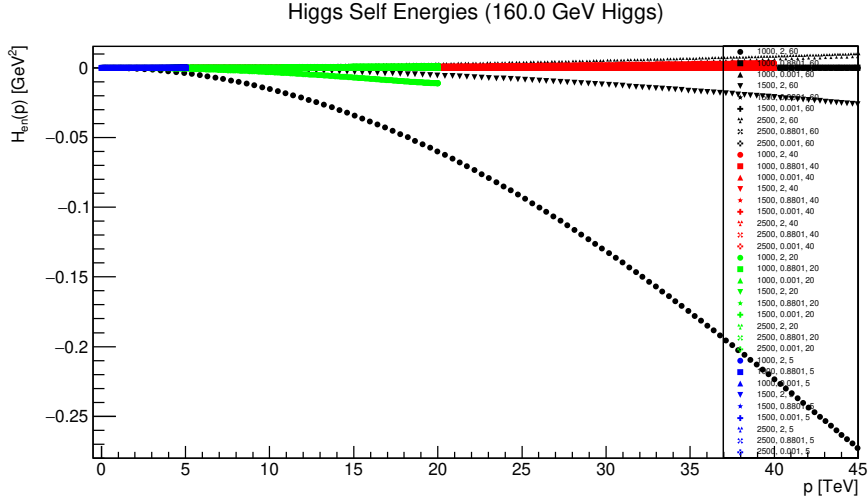


Figure 20: Higgs self energies for  $m_h = 160.0$  GeV are plotted (in TeV regime) with  $1000 \text{ GeV} \leq m_s \leq 2500 \text{ GeV}$ ,  $0.001 \leq \lambda \leq 2.0$ , and  $5 \text{ TeV} \leq \Lambda \leq 60 \text{ TeV}$ , shown as  $(m_s, \lambda, \Lambda)$  on the figure.

such that the tree level structure is at least few orders of magnitude higher than them, rendering very small contributions which, thus, are not visible in the propagators given in 13, 14, 17, and 18. However, for various parameters the dependence is quantitatively insignificant and can practically be neglected in favor of the tree level contribution. Overall, as the contributions beyond tree level are significantly smaller than the tree level structure,

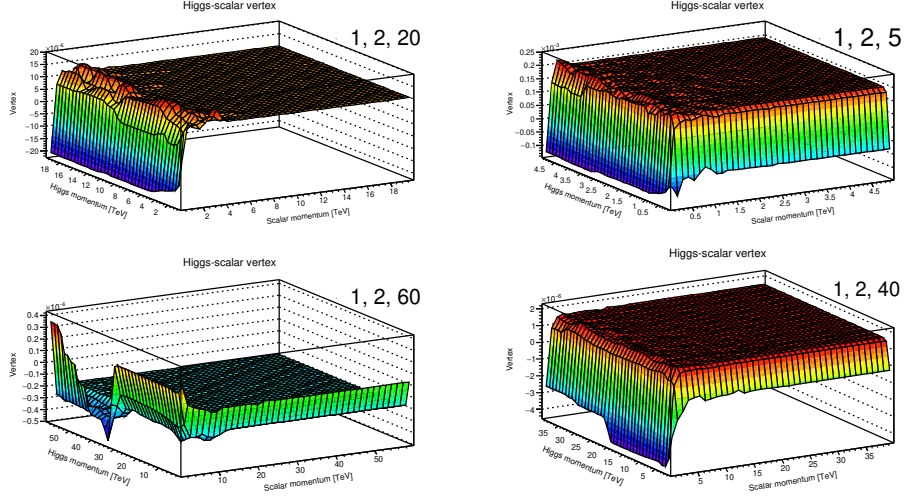


Figure 21: Higgs-scalar vertex for  $m_h = 125.09$  GeV,  $m_s = 1$  GeV, coupling  $\lambda = 2.0$ , for four cutoff values ( $\Lambda$ ) given in TeV. The figures are labelled as  $(m_s, \lambda, \Lambda)$ .

it favors perturbative picture which is also the case for the SM Higgs.

As for the case of scalar self energies, both positive and negative contributions from Higgs self energies are observed, though considerably smaller in comparison. However, a general observation is vanishing contributions as  $p^2 \rightarrow 0$  in contrast to scalar self energies.

Given the observed less sensitivity of Higgs propagators in parameter space as well as cutoff values, and that this behavior has already been observed in other studies, it is speculated that even if Higgs mass was not fixed at its physical mass it may not have improved sensitivity of Higgs propagators on the considered parameter region and the mass of Higgs would not have changed drastically from the bare mass value, particularly for a large bare mass value around electroweak scale, i.e.  $10^2$  GeV. However, at this point it is not clear what magnitude of contribution Higgs mass may receive in this case.

### 3.3 Higgs-scalar Vertex

As for Higgs and scalar fields Yukawa interaction vertex is the only means to interact (while not taking into account dynamic higher interaction vertices) in the model, it contains all the non-trivial features of the theory reported here. The vertex is defined in equation 11 (with  $\alpha = 0$ ) and are extracted

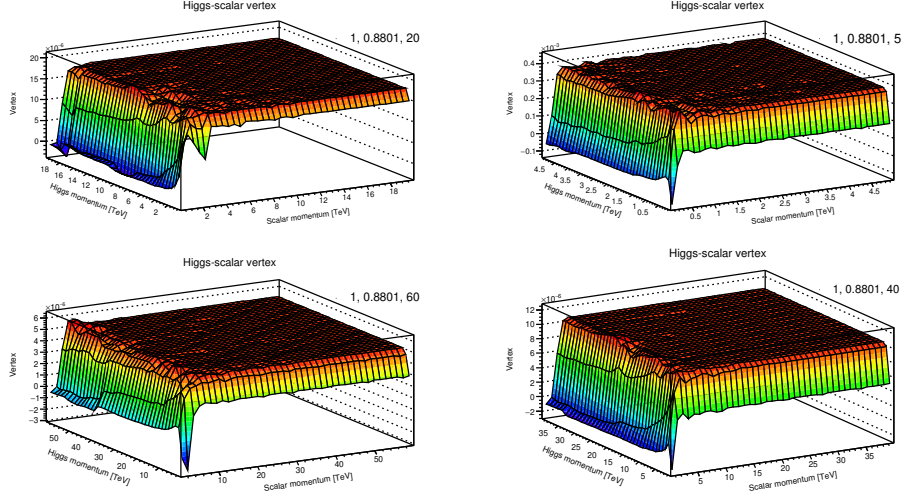


Figure 22: Higgs-scalar vertex for  $m_h = 125.09$  GeV,  $m_s = 1$  GeV, coupling  $\lambda = 0.8801$ , for four cutoff values ( $\Lambda$ ) given in TeV. The figures are labelled as  $(m_s, \lambda, \Lambda)$ .

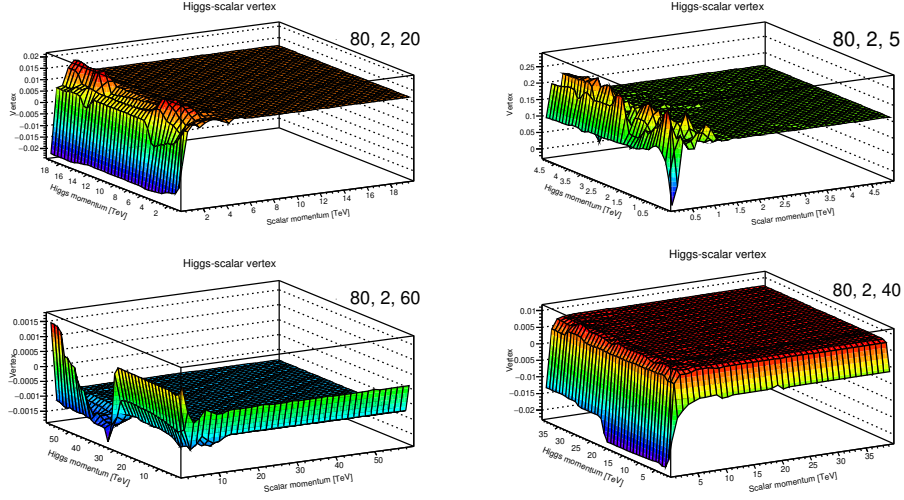


Figure 23: Higgs-scalar vertex for  $m_h = 125.09$  GeV,  $m_s = 80$  GeV, coupling  $\lambda = 2.0$ , for four cutoff values ( $\Lambda$ ) given in TeV. The figures are labelled as  $(m_s, \lambda, \Lambda)$ .

under the following condition <sup>11</sup>.

$$\tilde{\Gamma}^{ab}(u, -u - v, v)|_{u \rightarrow \Lambda, v \rightarrow \Lambda} = \lambda \quad (16)$$

<sup>11</sup>Note that the condition is not directly imposed on the renormalized vertex in equation 11.

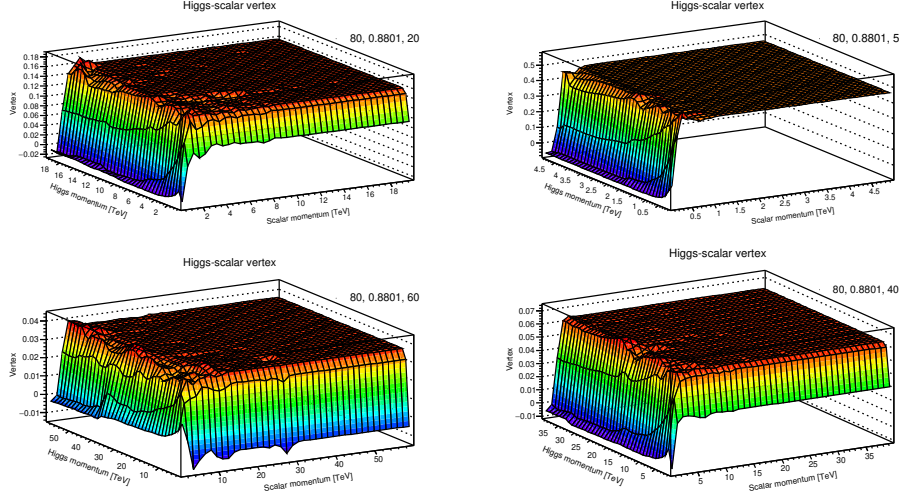


Figure 24: Higgs-scalar vertex for  $m_h = 125.09$  GeV,  $m_s = 80$  GeV, coupling  $\lambda = 0.8801$ , for four cutoff values ( $\Lambda$ ) given in TeV. The figures are labelled as  $(m_s, \lambda, \Lambda)$ .

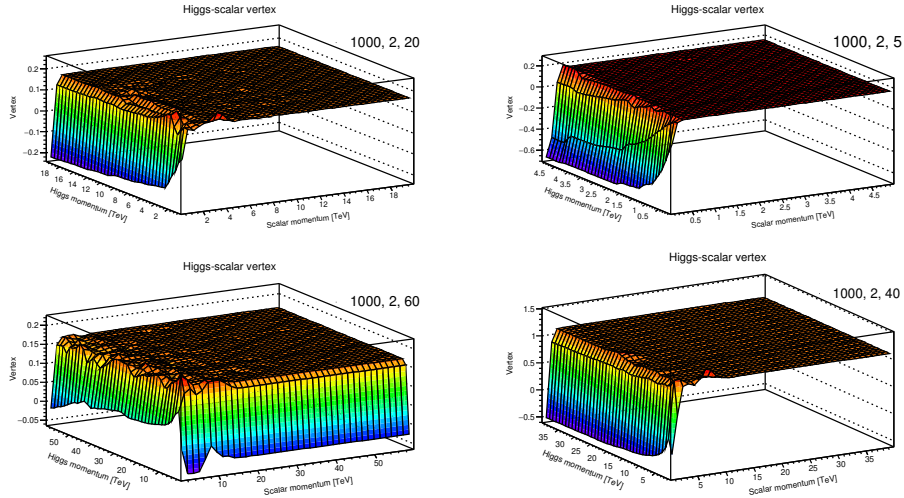


Figure 25: Higgs-scalar vertex for  $m_h = 125.09$  GeV,  $m_s = 1000$  GeV, coupling  $\lambda = 2.0$ , for four cutoff values ( $\Lambda$ ) given in TeV. The figures are labelled as  $(m_s, \lambda, \Lambda)$ .

The vertices are shown in figures 21 - 40 for various scalar (bare) masses and couplings for two Higgs masses at 4 cutoff values.

The first observation is that there are at least two types of vertices with distinct qualitative behavior. The first one is with formation of a 2-plateaus in which the vertex splits into two different regions such that in each region

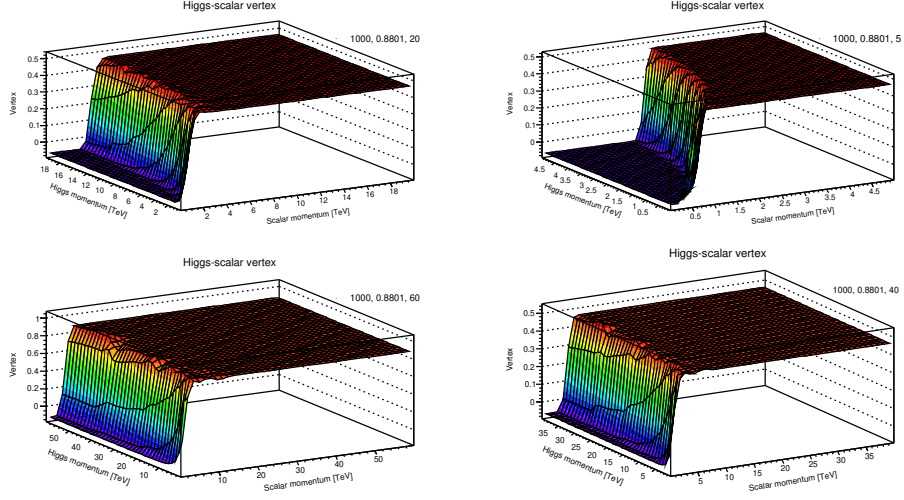


Figure 26: Higgs-scalar vertex for  $m_h = 125.09$  GeV,  $m_s = 1000$  GeV, coupling  $\lambda = 0.8801$ , for four cutoff values ( $\Lambda$ ) given in TeV. The figures are labelled as  $(m_s, \lambda, \Lambda)$ .

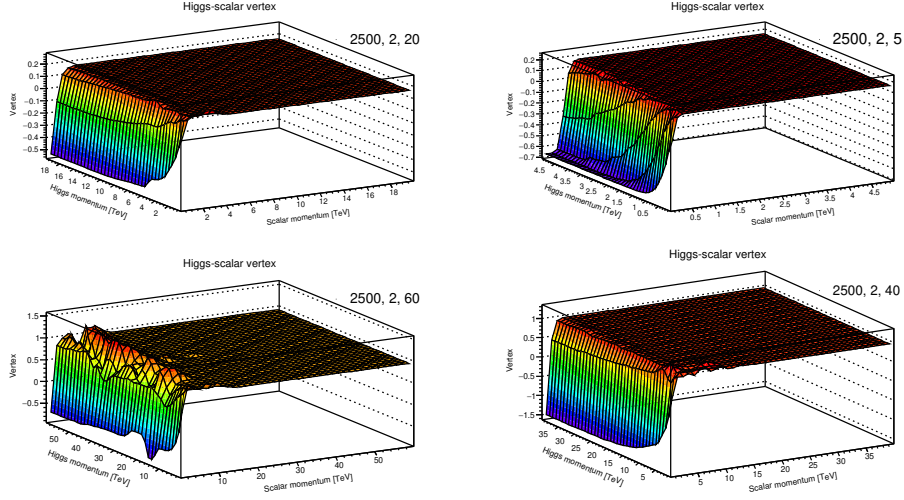


Figure 27: Higgs-scalar vertex for  $m_h = 125.09$  GeV,  $m_s = 2500$  GeV, coupling  $\lambda = 2.0$ , for four cutoff values ( $\Lambda$ ) given in TeV. The figures are labelled as  $(m_s, \lambda, \Lambda)$ .

the dependence on momentum is weak. The second type is a vertex which has no dependence on momentum over a wide region, and for one (or both) of the two) field momentum value(s) the vertex shows strong dependence in the corresponding low momentum region(s). However, a different version of the same type is a non-vanishing but distinctly suppressed vertices.



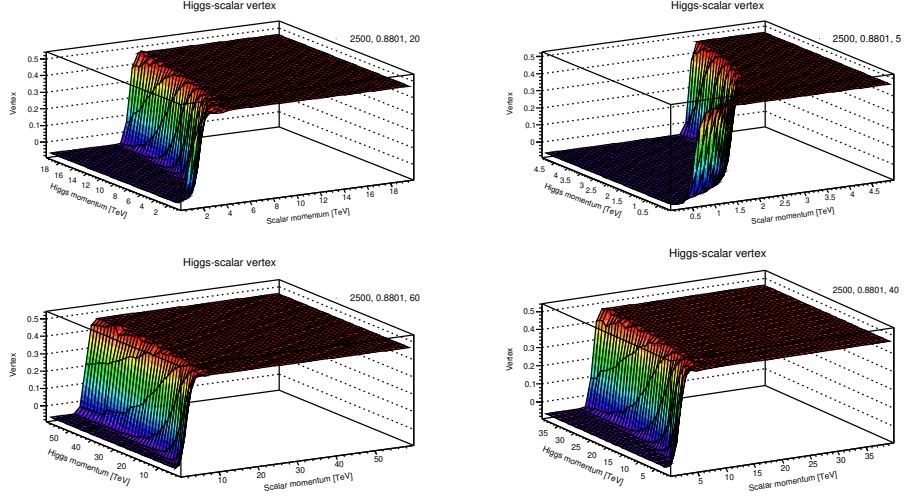


Figure 28: Higgs-scalar vertex for  $m_h = 125.09$  GeV,  $m_s = 2500$  GeV, coupling  $\lambda = 0.8801$ , for four cutoff values ( $\Lambda$ ) given in TeV. The figures are labelled as  $(m_s, \lambda, \Lambda)$ .

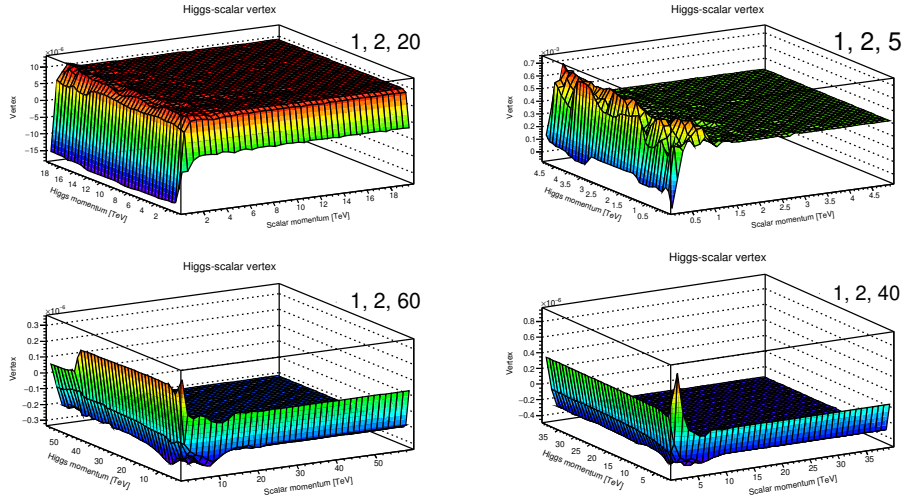


Figure 29: Higgs-scalar vertex for  $m_h = 160.0$  GeV,  $m_s = 1$  GeV, coupling  $\lambda = 2.0$ , for four cutoff values ( $\Lambda$ ) given in TeV. The figures are labelled as  $(m_s, \lambda, \Lambda)$ .

The 2-plateau behavior is frequently found for the case of scalar masses in TeV regime ( $m_s > 1$  TeV) with coupling values close to or greater than 1, particularly for small cutoff values. As the cutoff value is increased the 2-plateau behavior seems to gradually transform into the vertex which is mostly independent of field momentum values over most of the region, see

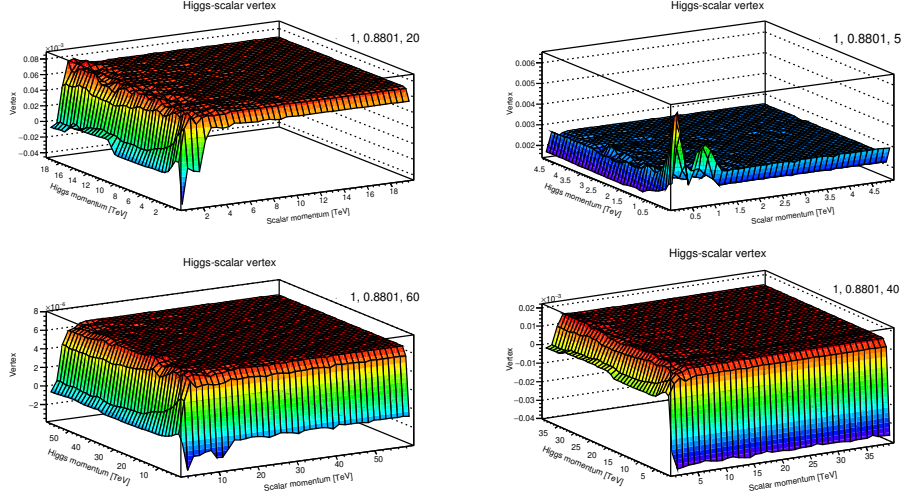


Figure 30: Higgs-scalar vertex for  $m_h = 160.0$  GeV,  $m_s = 1$  GeV, coupling  $\lambda = 0.8801$ , for four cutoff values ( $\Lambda$ ) given in TeV. The figures are labelled as  $(m_s, \lambda, \Lambda)$ .

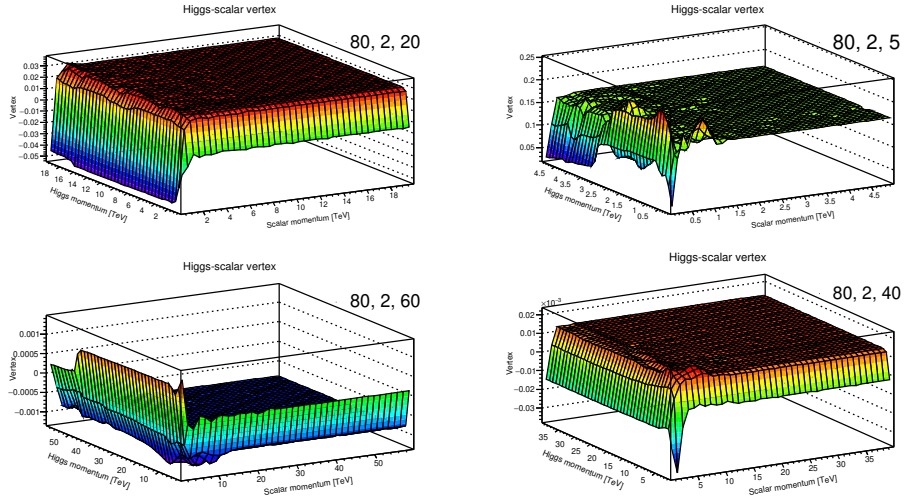


Figure 31: Higgs-scalar vertex for  $m_h = 160.0$  GeV,  $m_s = 80$  GeV, coupling  $\lambda = 2.0$ , for four cutoff values ( $\Lambda$ ) given in TeV. The figures are labelled as  $(m_s, \lambda, \Lambda)$ .

figures 27, 28, 35, and 36 for such a case, and figures 25, 26, 33, and 34 for relatively smaller scalar (bare) masses in TeV regime.

For low scalar masses in electroweak regime,  $m_s = 80$  GeV, the 2-plateau behavior is not found. However, there do exist some transitory vertices which are expected to exist between two regions in the parameter space with two



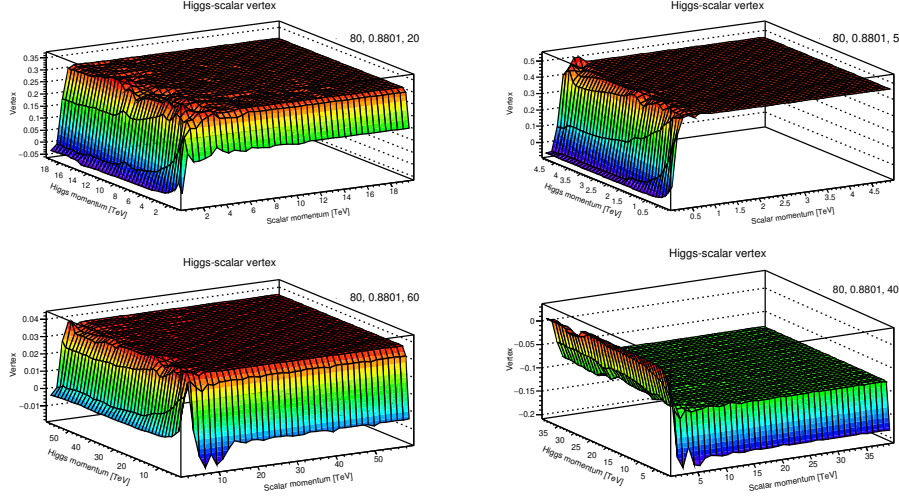


Figure 32: Higgs-scalar vertex for  $m_h = 160.0$  GeV,  $m_s = 80$  GeV, coupling  $\lambda = 0.8801$ , for four cutoff values ( $\Lambda$ ) given in TeV. The figures are labelled as  $(m_s, \lambda, \Lambda)$ .

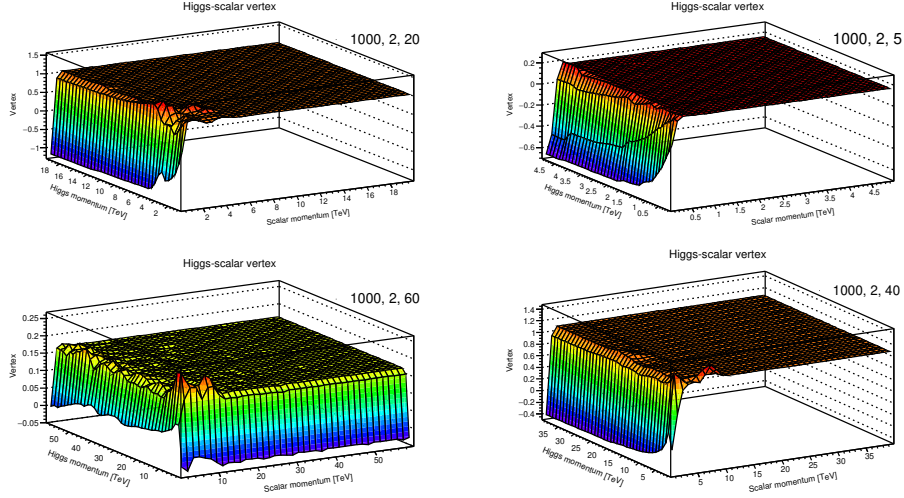


Figure 33: Higgs-scalar vertex for  $m_h = 160.0$  GeV,  $m_s = 1000$  GeV, coupling  $\lambda = 2.0$ , for four cutoff values ( $\Lambda$ ) given in TeV. The figures are labelled as  $(m_s, \lambda, \Lambda)$ .

different types of vertices. The parameters considered are mostly found in the region with vertices with weak dependence on momentum over majority of momentum values, see figures 23, 24, 31, and 32 for such a case.

For the lowest considered scalar mass ( $m_s = 1$  GeV), the vertices exhibit strongest dependence on Higgs mass. It is already expected as it is also the

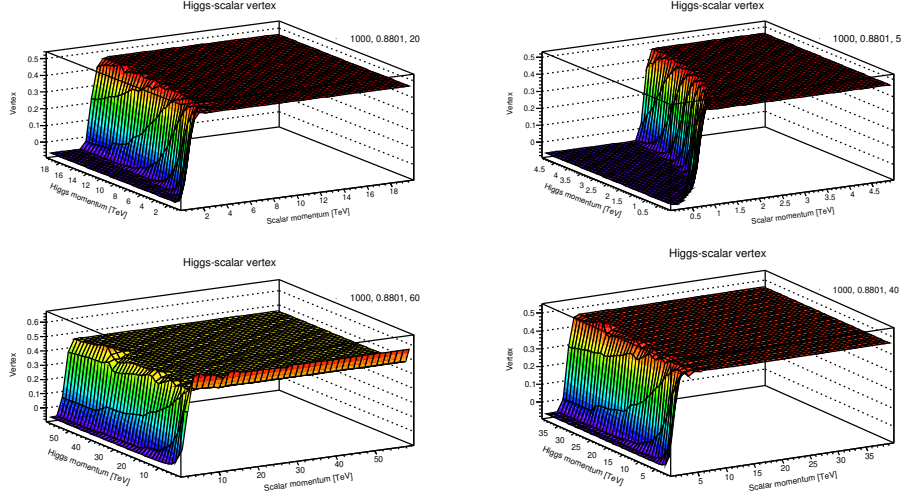


Figure 34: Higgs-scalar vertex for  $m_h = 160.0$  GeV,  $m_s = 1000$  GeV, coupling  $\lambda = 0.8801$ , for four cutoff values ( $\Lambda$ ) given in TeV. The figures are labelled as  $(m_s, \lambda, \Lambda)$ .

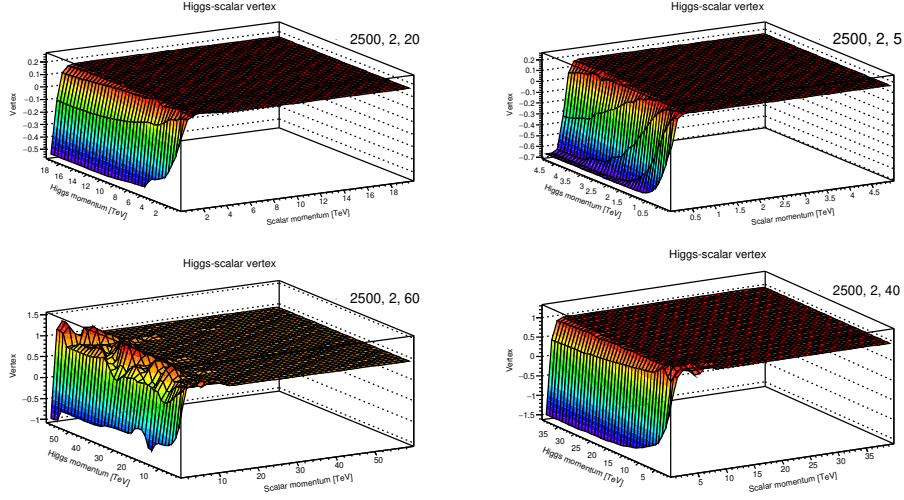


Figure 35: Higgs-scalar vertex for  $m_h = 160.0$  GeV,  $m_s = 2500$  GeV, coupling  $\lambda = 2.0$ , for four cutoff values ( $\Lambda$ ) given in TeV. The figures are labelled as  $(m_s, \lambda, \Lambda)$ .

region where scalar propagators and their corresponding self energies are found to have highly non-trivial behavior including the tendency of changing the sign of squared renormalized scalar mass. The vertices are mostly the ones with notable dependence on a particular end of momentum values, though it was observed that the momentum values over which momentum

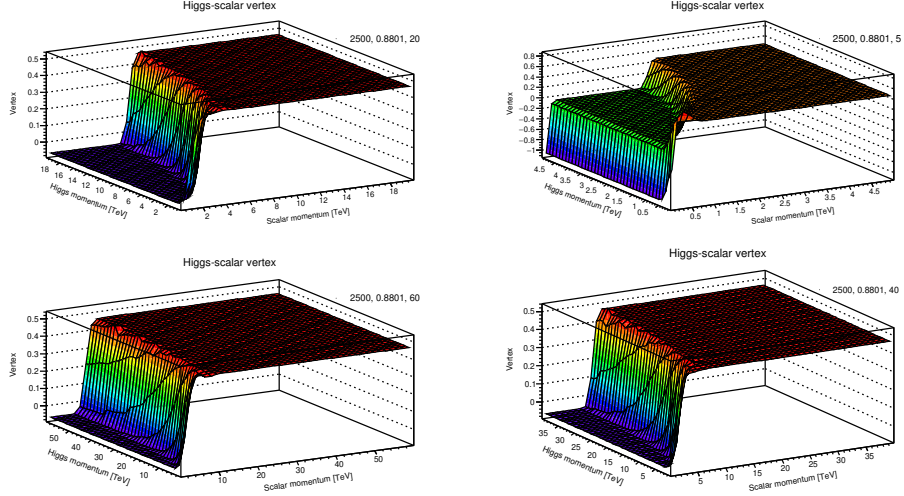


Figure 36: Higgs-scalar vertex for  $m_h = 160.0$  GeV,  $m_s = 2500$  GeV, coupling  $\lambda = 0.8801$ , for four cutoff values ( $\Lambda$ ) given in TeV. The figures are labelled as  $(m_s, \lambda, \Lambda)$ .

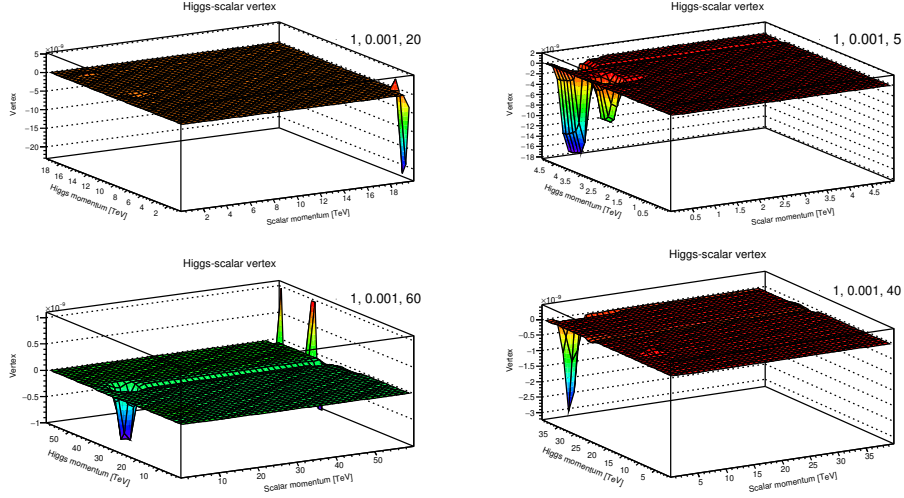


Figure 37: Higgs-scalar vertex for  $m_h = 125.09$  GeV,  $m_s = 1$  GeV, coupling  $\lambda = 0.001$ , for four cutoff values ( $\Lambda$ ) given in TeV. The figures are labelled as  $(m_s, \lambda, \Lambda)$ .

dependence arises is not the same for all the parameters, see figures 21, 22, 29, and 30. At this point, it is speculated to be a sign of a second order phase transformation.

A notable observation is that for the case of 2-plateau vertices no region is found with vanishing vertices. However, for the case of low coupling value,

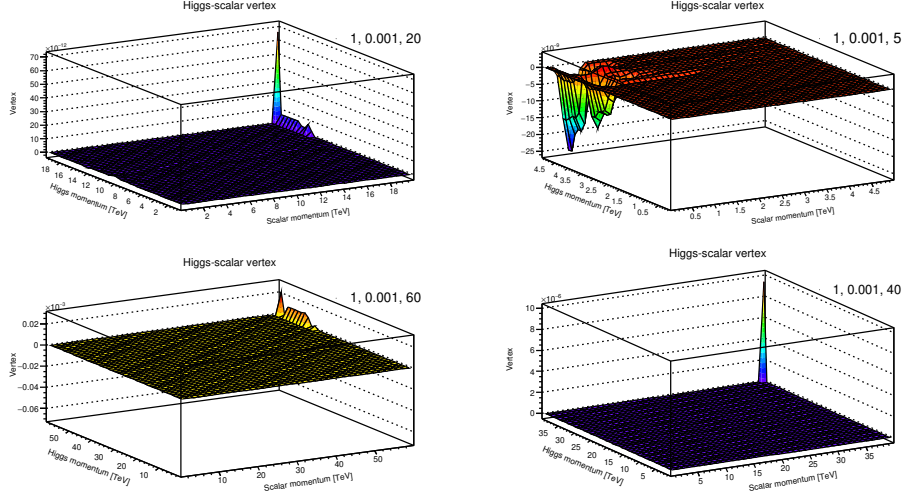


Figure 38: Higgs-scalar vertex for  $m_h = 160.0$  GeV,  $m_s = 1$  GeV, coupling  $\lambda = 0.001$ , for four cutoff values ( $\Lambda$ ) given in TeV. The figures are labelled as  $(m_s, \lambda, \Lambda)$ .

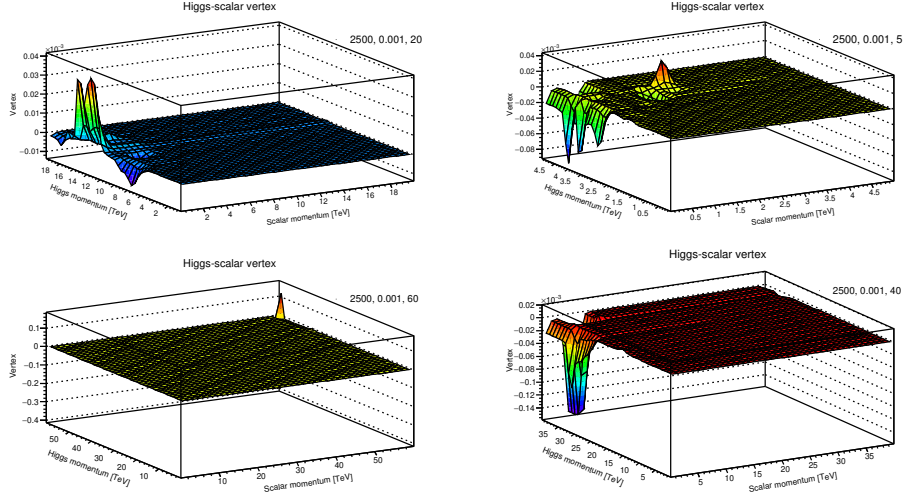


Figure 39: Higgs-scalar vertex for  $m_h = 125.09$  GeV,  $m_s = 2500$  GeV, coupling  $\lambda = 0.001$ , for four cutoff values ( $\Lambda$ ) given in TeV. The figures are labelled as  $(m_s, \lambda, \Lambda)$ .

$\lambda = 0.001$  in our case, the vertices have no significant dependence on most of the momentum values, particularly for higher cutoff values. Such vertices are also found to be strongly suppressed, though many orders larger than numerical precision. It indicates that the theory can still be taken as non-trivial. It was also observed that the suppression does not occur due to the

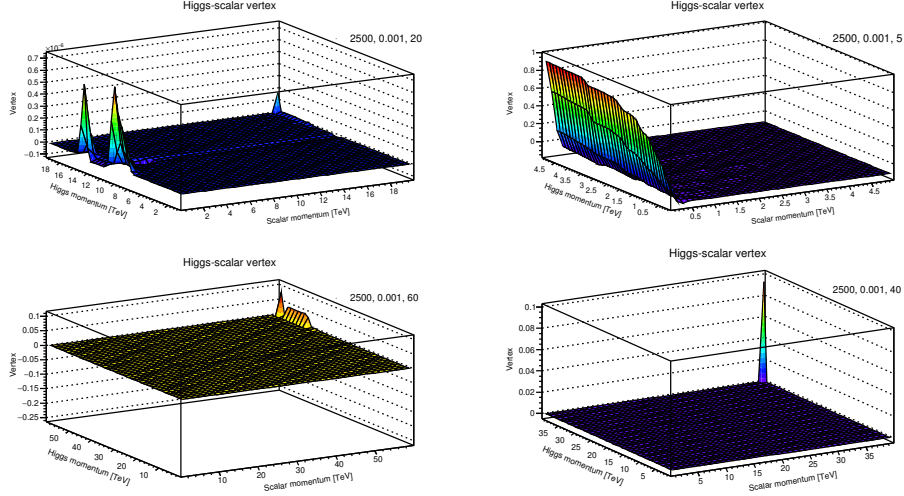


Figure 40: Higgs-scalar vertex for  $m_h = 160.0$  GeV,  $m_s = 2500$  GeV, coupling  $\lambda = 0.001$ , for four cutoff values ( $\Lambda$ ) given in TeV. The figures are labelled as  $(m_s, \lambda, \Lambda)$ .

condition imposed on the quantity  $\tilde{\Gamma}(u, -u - v, v)$  in equation 16. Since this is the case for all the vertices at  $\lambda = 0.001$ , only the vertices at  $m_s = 1$  GeV and  $m_s = 2500$  GeV are included in figures 37 to 40. However, this effect is found to become milder as the coupling is further lowered, and the significant difference between the condition imposed in the ultraviolet region and the magnitude of the vertex in the vicinity decreases.

A peculiar observation is that there is a trend of suppression of the vertices as the cutoff is increased, which can be observed in most of the shown vertices. However, there is a notable deviation from this behavior for case of 2-plateau vertices. It also tends to further support the classification of vertices and, possibly, a phase structure in the parameter space.

Furthermore, as the definition of the vertex in equation 11 involves contributions of a parameter as well as  $\tilde{\Gamma}(u, -u - v, v)$ , and the condition in equation 16 is not directly imposed on the vertex, the sensitive behavior of such contributions appear as the void of a clear pattern of the vertices.

Lastly, as several vertices are also observed which do not completely belong of one of the two classifications of the vertices, it suggests a possibility of a second order phase transition in the phase space, if there is indeed a phase structure in the theory. It is not a surprise in physics involving Higgs interactions as such a behavior has already been found in other studies involving Higgs interactions, see [65] for instance.



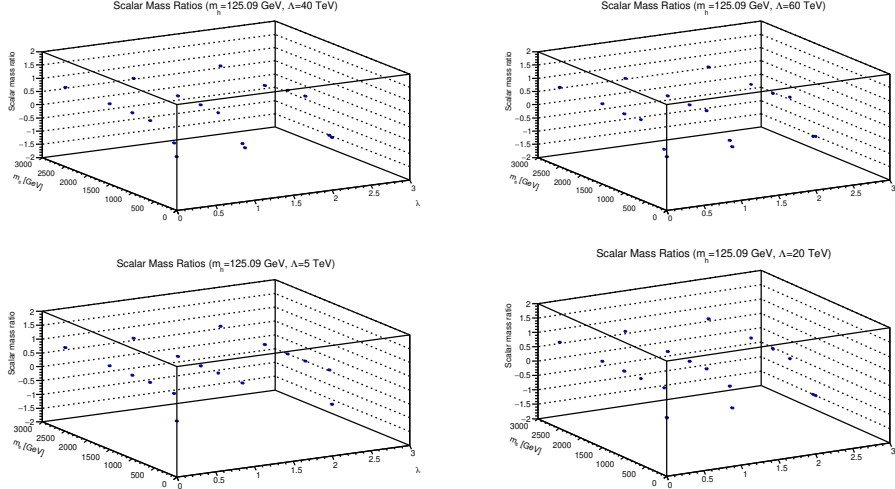


Figure 41: Scalar mass squared ratios ( $\frac{m_{s,r}^2}{m_s^2}$ ) for various couplings and scalar (bare) masses, for different cutoff values, are plotted for  $m_h = 125.09$  GeV.

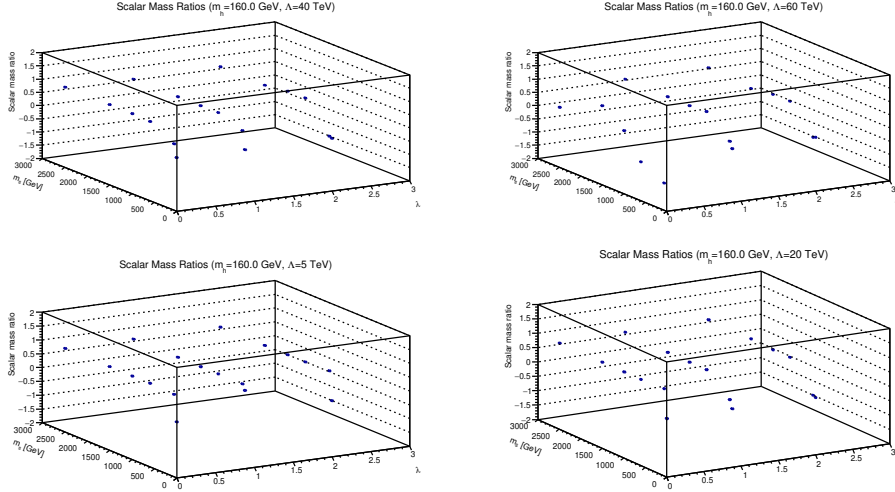


Figure 42: Scalar mass squared ratios ( $\frac{m_{s,r}^2}{m_s^2}$ ) for various couplings and scalar (bare) masses, for different cutoff values, are plotted for  $m_h = 160.0$  GeV.

### 3.4 Renormalized Masses

From the perspective of phenomenology and measurements, renormalized masses are among the most important features of the theory. The (squared) renormalized mass for scalar field, using equations 10 for B parameter are

given as

$$m_{s,r}^2 = (1 + A)(m_s^2 + 2\lambda\sigma_s) \quad (17)$$

while Higgs' mass is kept fixed, as mentioned before.

Results for scalar masses are shown in figures 41 and 42 for  $m_h = 125.09$  GeV and  $m_h = 160.0$  GeV, respectively, at various cutoff values, against several scalar bare masses and couplings. Ratios between squared renormalized scalar mass and the corresponding bare squared scalar mass are plotted in the figures.

For the case of  $m_h = 125.09$  GeV, a general observation is that for higher scalar masses the ratio is close to 1, indicating absence of significant beyond tree level contributions to physical scalar mass. It is understandable as it is already known that heavier masses usually have smaller contributions beyond the bare mass values in quantum field theories. The ratio is not found to have any significant dependence on couplings in this region.

However, for smaller values of  $m_s$  an interesting observation is suppression of the ratio which is the result of significant negative contributions from Yukawa interaction in the model. It supports the speculation made in section 3.1 regarding negative renormalized squared scalar masses. Furthermore, for higher cutoff values the effect is more pronounced towards small values ( $m_s < 80$  GeV) of scalar bare mass.

For heavier Higgs case, the quantitative behavior of the ratio is similar, see figure 42. It points towards the possibility that at least the Higgs mass at around electroweak scale might not effect scalar masses.

## 4 Conclusion

In this paper, results from a systematic studies of Wick Cutkosky's model with a three point Yukawa interaction among Higgs, Higgs bar, and scalar singlet fields are reported. The studies is a part of understanding richer renormalizable quantum field theories with flat background and investigating their phenomenology with minimum truncations and ansatz. Even in the presence of only one three point interaction vertex, the model considered is found to posses a number of non-trivial features.

Higgs propagators are found to have the simplest features. The propagators are quantitatively, as well as qualitatively, very close to each other for all explored cutoff and parameters. It raises an speculation that even if the Higgs mass was not fixed to its experimentally known value, it would not change the renormalized mass drastically in this model. The speculation also finds support for the case of the SM and some studies involving Higgs interactions. Hence, the model itself is found to be in harmony to current understanding about Higgs interactions.

However, scalar propagators do manifest themselves in some variety in the region of the explored parameter space. It was observed that in the

infrared region, they tend to draw a classification which was chosen in the paper. However, a more important feature is their diversity for low bare mass regions where the physical scalar masses receive significant contributions during renormalization procedure. The most important observation is negative contributions which have tendency to flip the sign of the physical squared mass, which may also be taken as a sign of symmetry breaking in the theory. Hence, the model contains signs of symmetry breaking even when Higgs squared mass is set at positive values and, hence, classically we are away from the region of Higgs mechanism in parameter space. It warrants an investigation of dynamic mass generation in the model. For higher bare scalar masses, such a breaking is not found as the physical masses are very close to the bare masses in the theory due to low beyond tree level contributions.

Another interesting feature of the theory is the presence of two types of vertices in terms of their dependence on field momentum, along with transitory vertices. The presence of such transitory vertices suggests a possibility of a second order transition, in case there is any phase structure in the model. However, this matter requires further studies of the theory, particularly in terms of spectroscopy of the theory.

Despite relatively strong suppression of vertices for some parameters, the theory can still be taken as a non-trivial theory, hence the model considered serves as an addition to evidence in favor of non-triviality of scalar interactions.

## 5 Acknowledgment

I am extremely thankful to Dr. Shabbar Raza for a number of important advices and valuable discussions throughout the endeavor. I would also like to thank Dr. Babar A. Qureshi for discussions in the early phase of this work, Prof. Holger Gies for valuable suggestions during writing of the manuscript, and my PhD adviser Prof. Axel Maas for introducing DSE approach to me in the first place.

This work was supported by faculty research grant from Habib University Karachi Pakistan, Lahore University of Management Sciences Pakistan, and partially supported by National Center for Physics Quaid-i-Azam University Islamabad Pakistan.

## References

- [1] J. Beringer et al. (Particle Data Group). *Phys. Rev. D*, 86:010001, 2012.
- [2] Axel Maas. Brout-Englert-Higgs physics: From foundations to phenomenology. 2017.



- [3] Marcela Carena and Howard E. Haber. Higgs boson theory and phenomenology. *Prog. Part. Nucl. Phys.*, 50:63–152, 2003.
- [4] Matthew D. Schwartz. *Quantum Field Theory and the Standard Model*. Cambridge University Press, 2014.
- [5] M. Kaku. *Quantum field theory: A Modern introduction*. 1993.
- [6] R. Michael Barnett et al. Particle physics summary. *Rev. Mod. Phys.*, 68:611–732, 1996.
- [7] Georges Aad et al. Observation of a new particle in the search for the Standard Model Higgs boson with the ATLAS detector at the LHC. *Phys. Lett.*, B716:1–29, 2012.
- [8] Serguei Chatrchyan et al. Observation of a new boson at a mass of 125 GeV with the CMS experiment at the LHC. *Phys. Lett.*, B716:30–61, 2012.
- [9] Stephen P. Martin. A Supersymmetry primer. 1997. [Adv. Ser. Direct. High Energy Phys.18,1(1998)].
- [10] V. Mukhanov. *Physical Foundations of Cosmology*. Cambridge University Press, Oxford, 2005.
- [11] Alan H. Guth. The Inflationary Universe: A Possible Solution to the Horizon and Flatness Problems. *Phys. Rev.*, D23:347–356, 1981.
- [12] John R. Ellis and Douglas Ross. A Light Higgs boson would invite supersymmetry. *Phys. Lett.*, B506:331–336, 2001.
- [13] John R. Ellis, Giovanni Ridolfi, and Fabio Zwirner. Higgs Boson Properties in the Standard Model and its Supersymmetric Extensions. *Comptes Rendus Physique*, 8:999–1012, 2007.
- [14] Gerard Jungman, Marc Kamionkowski, and Kim Griest. Supersymmetric dark matter. *Phys. Rept.*, 267:195–373, 1996.
- [15] Howard E. Haber and Ralf Hempfling. Can the mass of the lightest Higgs boson of the minimal supersymmetric model be larger than  $m(Z)$ ? *Phys. Rev. Lett.*, 66:1815–1818, 1991.
- [16] John R. Ellis, Giovanni Ridolfi, and Fabio Zwirner. Radiative corrections to the masses of supersymmetric Higgs bosons. *Phys. Lett.*, B257:83–91, 1991.
- [17] Yasuhiro Okada, Masahiro Yamaguchi, and Tsutomu Yanagida. Upper bound of the lightest Higgs boson mass in the minimal supersymmetric standard model. *Prog. Theor. Phys.*, 85:1–6, 1991.

- [18] John R. Ellis, Gian Luigi Fogli, and E. Lisi. Supersymmetric Higgses and electroweak data. *Phys. Lett.*, B286:85–91, 1992.
- [19] Morad Aaboud et al. Search for photonic signatures of gauge-mediated supersymmetry in 13 TeV  $pp$  collisions with the ATLAS detector. 2018.
- [20] Morad Aaboud et al. Search for electroweak production of supersymmetric states in scenarios with compressed mass spectra at  $\sqrt{s} = 13$  TeV with the ATLAS detector. *Submitted to: Phys. Rev. D*, 2017.
- [21] Alexei A. Starobinsky. A New Type of Isotropic Cosmological Models Without Singularity. *Phys. Lett.*, 91B:99–102, 1980.
- [22] K. Sato. First Order Phase Transition of a Vacuum and Expansion of the Universe. *Mon. Not. Roy. Astron. Soc.*, 195:467–479, 1981.
- [23] Vera-Maria Enckell, Kari Enqvist, Syksy Rasanen, and Eemeli Tomberg. Higgs inflation at the hilltop. 2018.
- [24] Fedor Bezrukov. The Higgs field as an inflaton. *Class. Quant. Grav.*, 30:214001, 2013.
- [25] J. G. Ferreira, C. A. de S. Pires, J. G. Rodrigues, and P. S. Rodrigues da Silva. Inflation scenario driven by a low energy physics inflaton. *Phys. Rev.*, D96(10):103504, 2017.
- [26] Rmi Hakim. The inflationary universe : A primer. *Lect. Notes Phys.*, 212:302–332, 1984.
- [27] Andrei D. Linde. Particle physics and inflationary cosmology. *Contemp. Concepts Phys.*, 5:1–362, 1990.
- [28] A. B. Lahanas, V. C. Spanos, and Vasilios Zarikas. Charge asymmetry in two-Higgs doublet model. *Phys. Lett.*, B472:119, 2000.
- [29] Vasilios Zarikas. The Phase transition of the two Higgs extension of the standard model. *Phys. Lett.*, B384:180–184, 1996.
- [30] Georgios Aliferis, Georgios Kofinas, and Vasilios Zarikas. Efficient electroweak baryogenesis by black holes. *Phys. Rev.*, D91(4):045002, 2015.
- [31] Vladimir B. Sauli. Nonperturbative solution of metastable scalar models: Test of renormalization scheme independence. *J. Phys.*, A36:8703–8722, 2003.
- [32] A. Hasenfratz, K. Jansen, J. Jersak, C. B. Lang, T. Neuhaus, and H. Yoneyama. Study of the Four Component  $\phi^4$  Model. *Nucl. Phys.*, B317:81–96, 1989.

- [33] F. Gliozzi. A Nontrivial spectrum for the trivial  $\lambda\phi^4$  theory. *Nucl. Phys. Proc. Suppl.*, 63:634–636, 1998.
- [34] Orfeu Bertolami, Catarina Cosme, and Joo G. Rosa. Scalar field dark matter and the Higgs field. *Phys. Lett.*, B759:1–8, 2016.
- [35] M. C. Bento, O. Bertolami, R. Rosenfeld, and L. Teodoro. Selfinteracting dark matter and invisibly decaying Higgs. *Phys. Rev.*, D62:041302, 2000.
- [36] C. P. Burgess, Maxim Pospelov, and Tonnies ter Veldhuis. The Minimal model of nonbaryonic dark matter: A Singlet scalar. *Nucl. Phys.*, B619:709–728, 2001.
- [37] M. C. Bento, O. Bertolami, and R. Rosenfeld. Cosmological constraints on an invisibly decaying Higgs boson. *Phys. Lett.*, B518:276–281, 2001.
- [38] Renata Jora.  $\Phi^4$  theory is trivial. *Rom. J. Phys.*, 61(3-4):314, 2016.
- [39] M. A. B. Beg and R. C. Furlong. The  $\Lambda\phi^4$  Theory in the Nonrelativistic Limit. *Phys. Rev.*, D31:1370, 1985.
- [40] Michael Aizenman. Proof of the Triviality of  $\phi^4$  Field Theory and Some Mean-Field Features of Ising Models for  $d \leq 4$ . *Phys. Rev. Lett.*, 47:886–886, 1981.
- [41] Roger F. Dashen and Herbert Neuberger. How to Get an Upper Bound on the Higgs Mass. *Phys. Rev. Lett.*, 50:1897, 1983.
- [42] Ulli Wolff. Precision check on triviality of  $\lambda\phi^4$  theory by a new simulation method. *Phys. Rev.*, D79:105002, 2009.
- [43] Peter Weisz and Ulli Wolff. Triviality of  $\phi_4^4$  theory: small volume expansion and new data. *Nucl. Phys.*, B846:316–337, 2011.
- [44] Johannes Siefert and Ulli Wolff. Triviality of  $\phi_4^4$  theory in a finite volume scheme adapted to the broken phase. *Phys. Lett.*, B733:11–14, 2014.
- [45] Matthijs Hogervorst and Ulli Wolff. Finite size scaling and triviality of  $\phi^4$  theory on an antiperiodic torus. *Nucl. Phys.*, B855:885–900, 2012.
- [46] Axel Maas and Tajdar Mufti. Two- and three-point functions in Landau gauge Yang-Mills-Higgs theory. *JHEP*, 04:006, 2014.
- [47] F. J. Dyson. The Radiation theories of Tomonaga, Schwinger, and Feynman. *Phys. Rev.*, 75:486–502, 1949.
- [48] Julian S. Schwinger. On the Green’s functions of quantized fields. 1. *Proc. Nat. Acad. Sci.*, 37:452–455, 1951.

- [49] Julian S. Schwinger. On the Green's functions of quantized fields. 2. *Proc. Nat. Acad. Sci.*, 37:455–459, 1951.
- [50] Eric S. Swanson. A Primer on Functional Methods and the Schwinger-Dyson Equations. *AIP Conf.Proc.*, 1296:75–121, 2010.
- [51] R. J. Rivers. *PATH INTEGRAL METHODS IN QUANTUM FIELD THEORY*. Cambridge University Press, 1988.
- [52] Morad Aaboud et al. Measurements of Higgs boson properties in the diphoton decay channel with  $36 \text{ fb}^{-1}$  of  $pp$  collision data at  $\sqrt{s} = 13$  TeV with the ATLAS detector. 2018.
- [53] M. Malbertion. SM Higgs boson measurements at CMS. *Nuovo Cim.*, C40(5):182, 2018.
- [54] Holger Gies, Ren Sondenheimer, and Matthias Warschinke. Impact of generalized Yukawa interactions on the lower Higgs mass bound. *Eur. Phys. J.*, C77(11):743, 2017.
- [55] Tajdar Mufti. Higgs-scalar singlet system with lattice simulations. *unpublished*.
- [56] Heinz J. Rothe. *Lattice Gauge Theories, An Introduction*. World Scientific, London, 1996. London, UK: world Scientific (1996) 381 p.
- [57] Tajdar Mufti. Phenomenology of Higgs-scalar singlet interactions. *unpublished*.
- [58] Jurij W. Darewych. Some exact solutions of reduced scalar Yukawa theory. *Can. J. Phys.*, 76:523–537, 1998.
- [59] E. Ya. Nugaev and M. N. Smolyakov. Q-balls in the WickCutkosky model. *Eur. Phys. J.*, C77(2):118, 2017.
- [60] J. W. Darewych and A. Duviryak. Confinement interaction in nonlinear generalizations of the Wick-Cutkosky model. *J. Phys.*, A43:485402, 2010.
- [61] A. Weber, J. C. Lopez Vieyra, Christopher R. Stephens, S. Dilcher, and P. O. Hess. Bound states from Regge trajectories in a scalar model. *Int. J. Mod. Phys.*, A16:4377–4400, 2001.
- [62] G. V. Efimov. On the ladder Bethe-Salpeter equation. *Few Body Syst.*, 33:199–217, 2003.
- [63] Craig D. Roberts and Anthony G. Williams. Dyson-Schwinger equations and their application to hadronic physics. *Prog. Part. Nucl. Phys.*, 33:477–575, 1994.

- [64] Tajdar Mufti. Two Higgs doublets with scalar mediations. *unpublished*.
- [65] Axel Maas and Tajdar Mufti. Spectroscopic analysis of the phase diagram of Yang-Mills-Higgs theory. *Phys. Rev.*, D91(11):113011, 2015.
- [66] Ashok Das. *Lectures on quantum field theory*. 2008.